THE METEOROLOGICAL MAGAZINE

HER MAJESTY'S
STATIONERY
OFFICE

March 1987

Met.O.978 No. 1376 Vol. 116

THE METEOROLOGICAL MAGAZINE

No. 1376, March 1987, Vol. 116

551.513.1:551.558.21

Linear models of stationary planetary waves forced by orography and thermal contrast*

G.J. Shutts

Meteorological Office, Bracknell

Summary

Time-averaged geopotential height maps are dominated by continental-scale long waves forced by orography and land/sea thermal asymmetry. Most of the energy associated with these longitudinal variations is contained in wave numbers 1–3 and extends from the surface to at least the upper stratosphere. Simple quasi-geostrophic theory on a beta-plane can be used to show how planetary waves forced near the surface can propagate to great heights as Rossby waves. Characteristic features of a solution representing the steady response to low-level heating can be identified in observations. These include a westward tilt with height of the wave system, poleward heat transport (particularly near the surface) and a 'whiplash' amplification of the disturbance in the stratosphere.

1. Introduction

By studying the dynamics of large-scale motion systems using linear theory one can effectively regard the weather chart (e.g. 500 mb contour height maps) as an interference pattern (as in wave optics) formed by the superposition of waves of different dynamical origin. Ultra-long wave motion (wavelengths greater than about 6000 km) is particularly amenable to this type of representation since global fields are readily expanded into complete sets of orthogonal functions (e.g. sines/cosines, Legendre functions and Hough functions). For instance, the broad character of the stratospheric circulation is well represented by a Fourier expansion in the zonal direction truncated at wave number 3, though this should not be interpreted as implying that higher wave numbers are dynamically unimportant. The linear approach ignores interactions between waves or between waves and zonally-averaged flow and so must be regarded as a gross approximation. Nevertheless, linearized solutions reveal much about the wave character of dynamical systems and provide a dynamically consistent model against which real data can be interpreted.

In sections 2 and 3 the Rossby wave as a three-dimensional motion system capable of transmitting energy and momentum over great distances in the atmosphere is considered. This involves the derivation of a wave equation for Rossby waves in a uniform westerly flow with constant static stability.

* Lecture note from a series of lectures entitled 'Dynamical Processes in Meteorology' given as part of the 1986 Advanced Lectures (Meteorological Office, 15 September–3 October 1986).

Conditions for wave propagation are established and the direction of energy propagation is linked to the group velocity. In sections 4 and 5 some steady responses of an airstream of uniform speed and direction to sinusoidal orography and fixed diabatic heat sources are obtained as analytical solutions to the quasi-geostrophic equations. The final section contains a comparison of the observed time-mean amplitude and phase of wave number 1 with the thermally-forced response given by the theory.

2. Quasi-geostrophic theory

The quasi-geostrophic vorticity equation on a mid-latitude beta-plane may be written as

$$\frac{\mathrm{D}}{\mathrm{D}t_{\mathrm{H}}}\zeta_{\mathrm{g}} + \beta v_{\mathrm{g}} = \frac{f_0}{\rho_0}\frac{\partial}{\partial z}(\rho_0 w) \qquad \ldots\ \ldots\ \ldots\ \ldots\ \ldots\ \ldots\ (1)$$

where ζ_{g} is the vertical component of the geostrophic vorticity vector, u_{g} and v_{g} are the components of the geostrophic wind, f_0 is a constant mid-latitude Coriolis parameter, β is the mean meridional gradient of the Coriolis parameter, $\rho_0(z)$ is the basic state density field (taken here to be proportional to $\exp(-z/H_0)$ where H_0 is the density scale height) and w is the vertical velocity. Also, the substantial derivative $\mathrm{D}/\mathrm{D}t_{\mathrm{H}}$ is given by

$$\frac{\mathrm{D}}{\mathrm{D}t_{\mathrm{H}}} = \frac{\partial}{\partial t} + u_{\mathrm{g}}\frac{\partial}{\partial x} + v_{\mathrm{g}}\frac{\partial}{\partial y}\,.$$

The geostrophic wind vector and vorticity are related to the perturbation pressure field p' (defined as the deviation of the pressure from the basic state $p_0(z)$) by

$$(u_{\mathrm{g}}, v_{\mathrm{g}}) = \frac{1}{f_0}\left\{-\frac{\partial}{\partial y}\left(\frac{p'}{\rho_0}\right), \frac{\partial}{\partial x}\left(\frac{p'}{\rho_0}\right)\right\} \qquad \ldots\ \ldots\ \ldots\ \ldots\ \ldots\ (2a)$$

$$\zeta_{\mathrm{g}} = \nabla_{\mathrm{H}}^2\left(\frac{p'}{\rho_0 f_0}\right) = \left(\frac{\partial^2}{\partial x^2} + \frac{\partial^2}{\partial y^2}\right)\frac{p'}{\rho_0 f_0}\,. \qquad \ldots\ \ldots\ \ldots\ \ldots\ \ldots\ (2b)$$

The geostrophic wind is approximated by its non-divergent, f-plane equivalent (based on f_0) in quasi-geostrophic theory.

Equation (1) tells us that the relative vorticity ζ_{g} can be changed by meridional advection with the geostrophic wind (βv_{g} term) and by the vertical stretching of planetary vorticity.

The thermodynamic equation may be expressed as

$$\frac{\mathrm{D}}{\mathrm{D}t_{\mathrm{H}}}\left(\frac{\theta'}{\theta_0}\right) + wB = S \qquad \ldots\ \ldots\ \ldots\ \ldots\ \ldots\ \ldots\ (3)$$

where θ' is the perturbation of the potential temperature from a horizontally stratified basic state $\theta_0(z)$, B is the static stability $1/\theta_0\ (\mathrm{d}\theta_0/\mathrm{d}z)$ and S is some unspecified diabatic heat source. Using the hydrostatic equation

$$\frac{\partial}{\partial z}\left(\frac{p'}{\rho_0}\right) = g\frac{\theta'}{\theta_0}$$

equation (3) may be written as

$$\frac{\mathrm{D}}{\mathrm{D}t_{\mathrm{H}}}\left\{\frac{\partial}{\partial z}\left(\frac{p'}{\rho_0}\right)\right\} + N^2 w = gS \qquad \ldots\ \ldots\ \ldots\ \ldots\ \ldots\ (4)$$

where g is the acceleration due to gravity and $N = (gB)^{1/2}$ is the Brunt-Väisälä frequency. By eliminating w

from equations (1) and (4), and substituting for (u_g, v_g) and ζ_g using the expressions in equations (2a) and (2b), a single equation for p' can be obtained and written as

$$\frac{D}{Dt_H}\left[\nabla_H^2 p' + \frac{\partial}{\partial z}\left\{\frac{\rho_0 f_0^2}{N^2}\frac{\partial}{\partial z}\left(\frac{p'}{\rho_0}\right)\right\}\right] + \beta\frac{\partial p'}{\partial x} = f_0^2 g\frac{\partial}{\partial z}\left(\frac{\rho_0 S}{N^2}\right) \quad \ldots\ \ldots\ (5)$$

with

$$\frac{D}{Dt_H} = \frac{\partial}{\partial t} + \frac{1}{f_0\rho_0}\left(\frac{\partial p'}{\partial x}\frac{\partial}{\partial y} - \frac{\partial p'}{\partial y}\frac{\partial}{\partial x}\right)$$

(cf. Gill (1982), page 530, equation (12.8.7) — the adiabatic case).

3. Free Rossby wave solutions

Consider now the special case of equation (5), where $N^2 =$ constant and $S = 0$, and linearize the equation about an atmosphere with uniform zonal wind U. This involves the substitution of $p' = -\rho_0 f_0 Uy + \delta p$, where δp is the pressure perturbation associated with the Rossby wave, and the neglect of terms quadratic in δp so that

$$\left(\frac{\partial}{\partial t} + U\frac{\partial}{\partial x}\right)\left[\nabla_H^2\delta p + \left(\frac{f_0}{N}\right)^2\frac{\partial}{\partial z}\left\{\rho_0\frac{\partial}{\partial z}\left(\frac{\delta p}{\rho_0}\right)\right\}\right] + \beta\frac{\partial}{\partial x}\delta p = 0. \quad \ldots\ \ldots\ (6)$$

Wave solutions to equation (6) have the form

$$\delta p = \mathrm{Re}\,[F(z)\exp\{\mathrm{i}(kx \pm \mu y - \sigma t)\}]$$

where $F(z)$ is a complex vertical structure function, k and μ are zonal and meridional wave numbers respectively, and σ is the angular frequency. Substituting this expression in equation (6) gives

$$(-\mathrm{i}\sigma + Uik)\left[-K^2F + \left(\frac{f_0}{N}\right)^2\frac{\mathrm{d}}{\mathrm{d}z}\left\{\rho_0\frac{\mathrm{d}}{\mathrm{d}z}\left(\frac{F}{\rho_0}\right)\right\}\right] + \beta ikF = 0$$

where $K^2 = \mathrm{k}^2 + \mu^2$. This further simplifies to

$$\frac{\mathrm{d}^2F}{\mathrm{d}z^2} + \frac{1}{H_0}\frac{\mathrm{d}F}{\mathrm{d}z} + \left\{\left(\frac{N}{f_0}\right)^2\frac{\beta}{U-c} - K^2\right\}F = 0 \quad \ldots\ \ldots\ \ldots\ \ldots\ (7)$$

where $c = \sigma/k$ is the phase speed. It is easily verified that $F(z)$ has solutions of the form

$$F(z) = \exp\left(\mathrm{i}\nu z - \frac{z}{2H_0}\right)$$

where ν is a vertical wave number given by the dispersion relation

$$\nu^2 + \frac{1}{4H_0^2} = \left(\frac{N}{f_0}\right)^2\left(\frac{\beta}{U-c} - K^2\right). \quad \ldots\ \ldots\ \ldots\ \ldots\ \ldots\ (8)$$

A linear combination of solutions of the form

$$\delta p = \exp\left\{\mathrm{i}(kx \pm \mu y \pm \nu z - \sigma t) - \frac{z}{2H_0}\right\}$$

will satisfy equation (6) (different combinations of + and − are used). Note that if ν^2 is positive, ν is a real quantity and the solutions will be wave-like in the vertical as well as the horizontal. Otherwise, ν would

be a pure imaginary number and δp would be given by

$$\delta p = \exp\left\{ \mathrm{i}(kx \pm \mu y) \pm |\nu| z - \frac{z}{2H_0} \right\}.$$

It is instructive to calculate the kinetic energy per unit volume $\frac{1}{2}\rho_0 (u_g^2 + v_g^2)$ averaged over a horizontal wavelength in the zonal and meridional directions. When $\nu^2 > 0$ this is easily shown to be a constant, otherwise

$$\tfrac{1}{2}\rho_0 (u_g^2 + v_g^2) \propto \exp(\pm 2|\nu| z)$$

and the energy grows or decays exponentially with height. Therefore it is physically reasonable to reject the solution with $\nu = -\mathrm{i}|\nu|$ corresponding to $\nu^2 < 0$ since the energy source for the disturbance cannot originate at infinite height.

The condition $\nu^2 > 0$ may be re-expressed as

$$K^2 < \left(\frac{\beta}{U-c} - \frac{f_0^2}{4H_0^2 N^2} \right) \quad \ldots\ldots\ldots\ldots\ldots\ldots (9)$$

or

$$0 < U-c < \frac{\beta}{K^2 + \left(\frac{f_0}{N}\right)^2 \frac{1}{4H_0^2}} \quad \ldots\ldots\ldots\ldots\ldots (10)$$

and was first put forward by Charney and Drazin (1961). The conditions given by equations (9) and (10) suggest that only the largest horizontal scales of wave motion will be capable of propagating vertically and that strong westerly winds may act as a barrier to Rossby wave energy. Note also that for stationary waves ($c = 0$) vertical energy propagation is impossible in easterly winds. Figs 1 and 2 show geopotential height and temperature maps of the 10 mb pressure surface for winter and summer in the northern hemisphere. The westerly zonal circulation in winter allows planetary wave energy (typically only wave numbers 1 and 2) to propagate from the troposphere up to the mesosphere so that the time-averaged stratospheric circulation exhibits persistent features such as the Aleutian High. In contrast, the easterly summer-time regime of the stratosphere is opaque to upward propagating stationary planetary waves and the flow is extremely zonal.

Setting $\mu = 0$ for convenience, it can be shown that wave solutions of the form

$$\delta p \propto \exp\left\{ \mathrm{i}(kx + \nu z - \sigma t) - \frac{z}{2H_0} \right\} \quad \ldots\ldots\ldots\ldots\ldots (11)$$

transmit disturbance energy upwards and since their lines of constant phase are given by $kx + \nu z - \sigma t$ equal to a constant, they tilt upstream with height (Fig. 3). In fact it is this type of solution which is most relevant to the real atmosphere since the principal energy sources for these waves are found in the lower troposphere and their upward propagation is unimpeded — even by the sudden change in static stability at the tropopause.

The dispersion relation equation (8) can be re-expressed in terms of σ yielding

$$\sigma = Uk - \frac{\beta k}{K^2 + \left(\frac{f_0}{N}\right)^2 \left(\nu^2 + \frac{1}{4H_0^2}\right)}$$

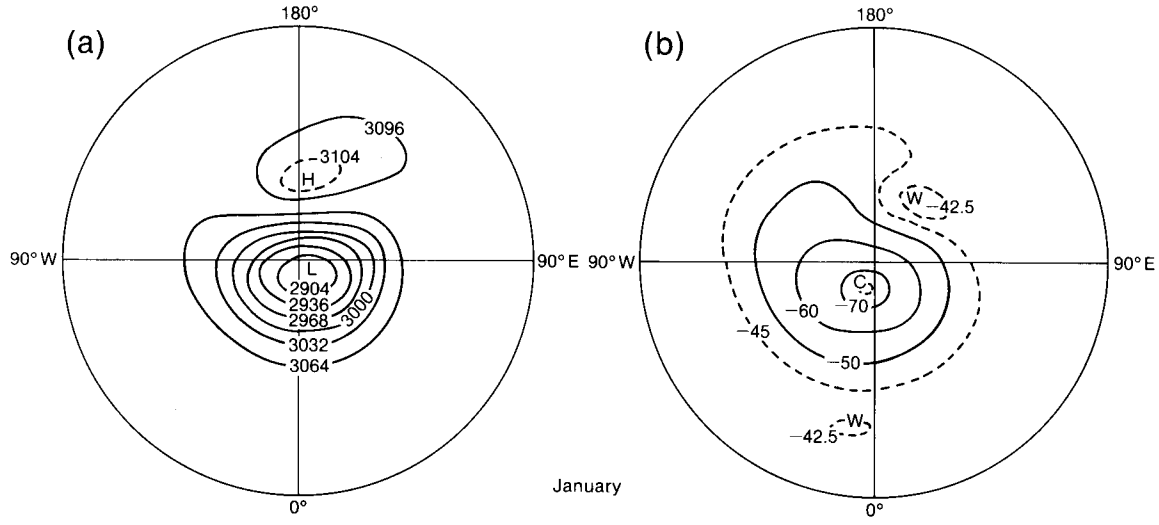

Figure 1. Synoptic charts at 10 mb for the northern hemisphere in January showing fields of (a) geopotential height (dam) and (b) temperature (°C) averaged over several years.

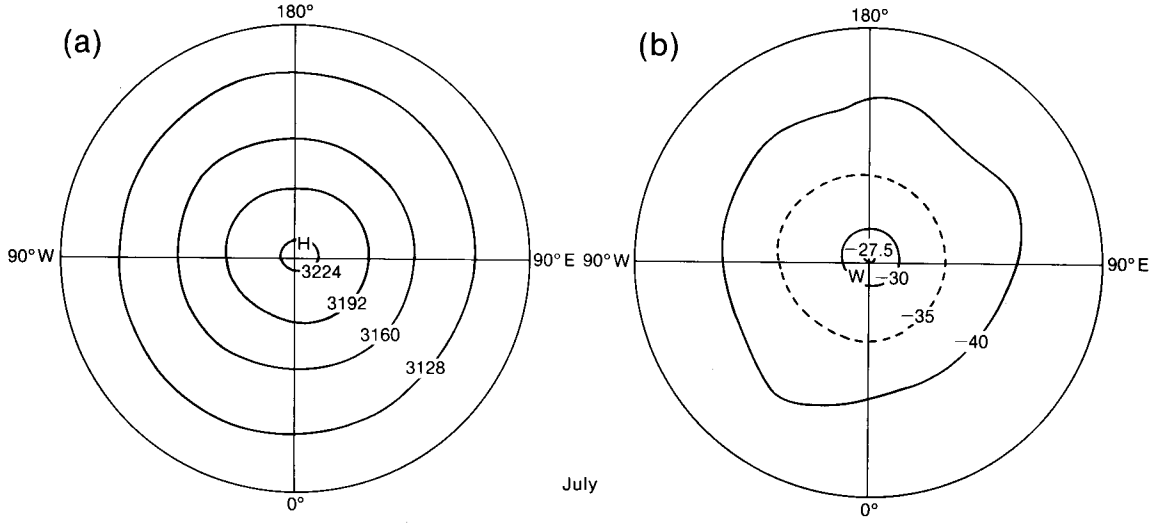

Figure 2. As Fig. 1 but for July.

and the vertical component of the group velocity (C_{gz}), which represents the speed and direction of energy propagation, can be obtained by differentiating with respect to ν giving

$$C_{gz} = \frac{\partial \sigma}{\partial \nu} = \frac{2\beta k \left(\frac{f_0}{N}\right)^2 \nu}{\left\{ K^2 + \left(\frac{f_0}{N}\right)^2 \left(\nu^2 + \frac{1}{4H_0^2}\right)\right\}^2} \quad \ldots \ldots \ldots \ldots \ldots \quad (12)$$

Upward energy propagation ($C_{gz} > 0$) is then associated with $\nu > 0$ as selected for equation (11).

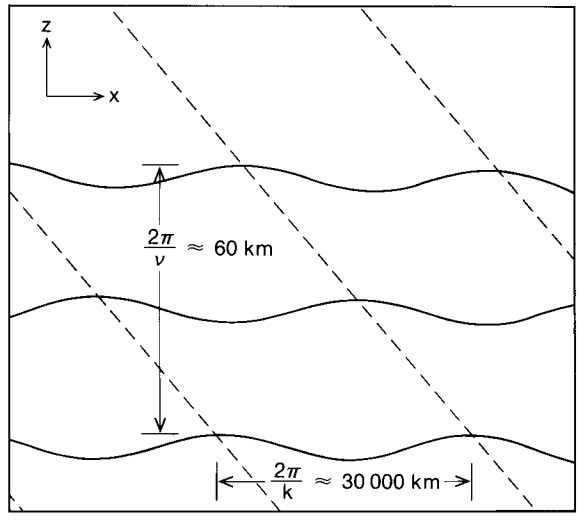

Figure 3. Phase lines of upward energy radiating planetary Rossby waves.

Alternatively, equation (12) can be written as

$$C_{gz} = \frac{2\beta k \left(\frac{f_0}{N}\right)^2 \nu}{\left(\frac{\beta}{U-c}\right)^2}$$

by making use of equation (8). If $K^2 << \beta/(U-c)$ and $1/(4H_0^2) << \nu^2$ then equation (8) gives

$$\nu^2 \approx \left(\frac{N}{f_0}\right)^2 \frac{\beta}{U-c}$$

and the expression for C_{gz} becomes

$$C_{gz} \approx \frac{2f_0 k}{N\beta^{1/2}} (U-c)^{3/2} . \quad \ldots \ldots \ldots \ldots \ldots \ldots (13)$$

Substituting typical values, e.g., $f = 10^{-4}$ s^{-1}, $k = 2\pi/(30\,000$ km), $N = 10^{-2}$ s^{-1}, $U-c = 10$ m s^{-1} and $\beta = 1.6 \times 10^{-11}$ m^{-1} s^{-1}, gives $C_{gz} \approx 3$ km/day suggesting a time-scale of about 1 week for wave number 1 disturbances forced near the surface to reach the stratosphere. Note also that even stationary waves ($c = 0$) are capable of transmitting disturbance energy upwards.

The free Rossby waves discussed in this section are really just a convenient device for establishing the dispersive properties of purely sinusoidal inviscid, adiabatic motion and are not a specific model of an atmospheric phenomenon.

Following is a description of specific time-independent solutions to equation (5) which relate stationary Rossby wave structure to particular forcing mechanisms. The general characteristics of these stationary solutions may be compared to the observed time-mean long-wave pattern, though quantitative agreement only implies the plausibility of the model not its accuracy.

4. Orographic planetary waves

Linearizing equation (5) about an atmosphere of uniform static stability and zonal wind gives

$$U\frac{\partial}{\partial x}\left[\nabla_{\mathrm{H}}^2\delta p + \frac{\partial}{\partial z}\left\{\rho_0\left(\frac{f_0}{N}\right)^2\frac{\partial}{\partial z}\left(\frac{\delta p}{\rho_0}\right)\right\}\right] + \beta\frac{\partial}{\partial x}\delta p = f_0^2\, g\frac{\partial}{\partial z}\left(\frac{\rho_0 S}{N^2}\right). \quad \ldots\ \ldots\ \ldots (14)$$

Stationary solutions to equation (14) with $S=0$ are easily obtainable for flow over a sinusoidal 'mountain' whose height $h(x, y)$ is given by

$$\begin{aligned} h(x, y) &= h_{\mathrm{m}} \sin kx \cos \mu y \\ &= h_{\mathrm{m}} \operatorname{Re}[-\mathrm{i}\exp(\mathrm{i}kx)\cos \mu y] \quad \ldots\ \ldots\ \ldots\ \ldots\ \ldots (15) \end{aligned}$$

where h_{m} is the height of the peak.

Linearizing the interface condition $w = \mathrm{D}h/\mathrm{D}t$ at $z=h$ gives $w = U(\partial h/\partial x)$ at $z=0$, which may be substituted into the linearized form of the thermodynamic equation (4) yielding

$$U\frac{\partial^2}{\partial x \partial z}\left(\frac{\delta p}{\rho_0}\right) + N^2 U\frac{\partial h}{\partial x} = 0$$

or

$$\frac{\partial}{\partial z}\left(\frac{\delta p}{\rho_0}\right) = -N^2 h(x, y) \quad \ldots\ \ldots\ \ldots\ \ldots\ \ldots\ \ldots (16)$$

at $z=0$.

The upward propagating stationary solutions are given by

$$\frac{\delta p}{\rho_0} = D\exp\left(\mathrm{i}\nu z + \frac{z}{2H_0} + \mathrm{i}kx\right)\cos \mu y$$

where D has to be determined from the lower boundary condition; equation (16) implies that

$$D\left(\mathrm{i}\nu + \frac{1}{2H_0}\right) = \mathrm{i}N^2 h_{\mathrm{m}}$$

or

$$D = \frac{N^2 h_{\mathrm{m}}\left(\nu + \frac{\mathrm{i}}{2H_0}\right)}{\nu^2 + \frac{1}{4H_0^2}}.$$

Consequently $\delta p/\rho_0$ is given by

$$\frac{\delta p}{\rho_0} = \operatorname{Re}\left[\frac{N^2 h_{\mathrm{m}}}{\nu^2 + \frac{1}{4H_0^2}}\left(\nu + \frac{\mathrm{i}}{2H_0}\right)\exp\left\{\mathrm{i}(\nu z + kx) + \frac{z}{2H_0}\right\}\right]\cos \mu y$$

or

$$\frac{\delta p}{\rho_0} = \frac{-h_{\mathrm{m}}N^2}{\left(\nu^2 + \frac{1}{4H_0^2}\right)^{1/2}}\sin(kx + \nu z - \delta)\exp\left(\frac{z}{2H_0}\right)\cos \mu y$$

where $\delta = \tan^{-1}(2H_0\nu)$. The phase difference between p'/ρ_0 and $h(x, y)$ at $z=0$ implies that the

planetary wave is exerting a drag force on the orography. Taking $h_m = 200$ m, $B = 3 \times 10^{-5}$ m^{-1}, $U = 10$ m s^{-1}, $k = 2\pi/(30\,000$ km) and $\mu = 2\pi/(12\,000$ km) (corresponding to one middle-latitude maximum in the meridional structure of the wave) gives a pressure perturbation δp of about 4 mb.

Since most of the terrain height variation is due to mountain ranges which are smaller in extent than the continental scale relevant to planetary waves, the significance of these solutions is rather questionable. In view of this uncertainty we shall proceed to the case of diabatically-forced long waves and their comparison with observations.

5. Stationary thermally-forced wave solutions

Differences in thermal energy budgets over land and sea lead to large zonal asymmetries in the diabatic heating rate averaged over, say, 1 month. In the northern hemisphere winter slow radiative cooling (about 1 K/day) dominates over continental interiors (e.g. Siberia) in marked contrast to flow over the oceans which experiences rapid heating (about 3 K/day) due to the vigorous transfer of sensible and latent heat from the sea (Fig. 4). Linear theory can be used to get some idea of the large-scale stationary wave response to zonally-asymmetric, time-averaged heat sources.

Consider the response of δp in equation (14) to a sinusoidal distribution of heating which decays exponentially with height, i.e.

$$S = a \sin kx \cos \mu y \exp(-bz)$$

or

$$S = \mathrm{Re}[-\mathrm{i}a \exp(\mathrm{i}kx - bz) \cos \mu y] \quad \ldots\ \ldots\ \ldots\ \ldots\ \ldots\ (17)$$

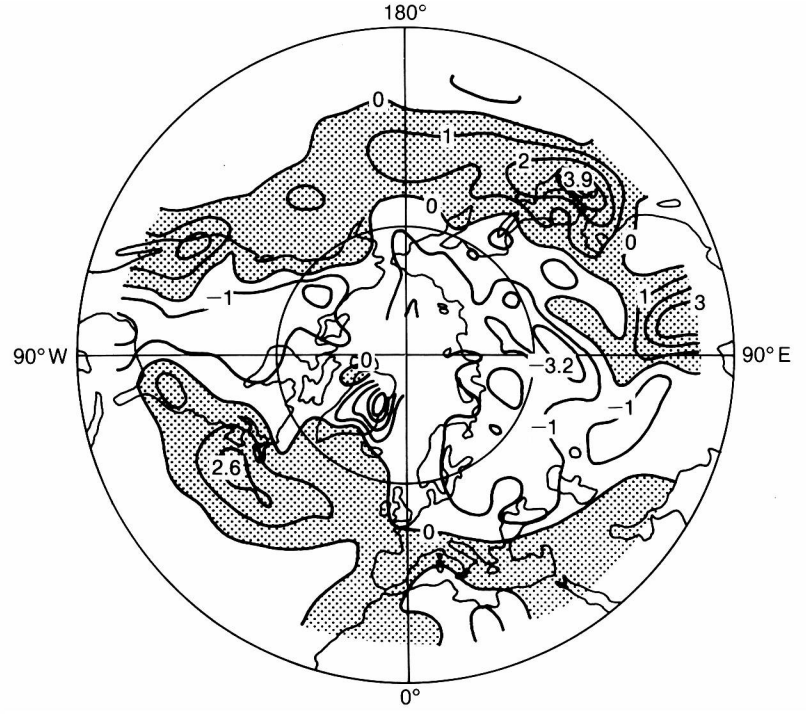

Figure 4. Diabatic heating computed for the 700 mb level in winter (contour interval 1 K/day) as estimated by Lau (1979). Shaded areas indicate regions of positive heating.

where a is a constant, k and μ are as defined previously and $1/b$ represents a depth scale for the diabatic source. The form of equation (17) suggests solutions of the kind

$$\delta p = \mathrm{Re}\,[F(z)\exp(\mathrm{i}kx)\cos\mu y] \quad \ldots\ \ldots\ \ldots\ \ldots\ \ldots\ (18)$$

where we expect $F(z)$ to be a complex function of z.

Substituting equations (17) and (18) into equation (14) leads to an ordinary differential equation for $F(z)$ as follows

$$\frac{\mathrm{d}}{\mathrm{d}z}\left\{\rho_0\frac{\mathrm{d}}{\mathrm{d}z}\left(\frac{F}{\rho_0}\right)\right\} + \frac{N^2}{f_0^2}\left(\frac{\beta}{U} - K^2\right)F = \frac{\rho_s a g}{Uk}\gamma\exp(-\gamma z) \quad \ldots\ \ldots\ \ldots\ (19)$$

where $\rho_s = \rho_0(z=0)$ and $\gamma = (b + 1/H_0)$. The general solution to this equation will involve a 'particular integral' which satisfies equation (19) on its own, together with a 'complementary function' which satisfies equation (19) when the right-hand side is zero (the homogeneous equation). The complementary function will in general involve two independent solutions to the homogeneous equation with multiplying factors to be determined by applying boundary conditions to the general solution.

Particular integrals of equation (19) will be of the form $C\exp(-\gamma z)$ and it can be shown that

$$C = \frac{\rho_s a g \gamma}{Uk\left\{bg + \left(\frac{N}{f_0}\right)^2\left(\frac{\beta}{U} - K^2\right)\right\}}.$$

The full solution will be of the form

$$\delta p = \mathrm{Re}\,[\{C\exp(-\gamma z) + \text{complementary function}\}\exp(\mathrm{i}kx)\cos\mu y] \quad \ldots\ \ldots\ \ldots\ (20)$$

and must satisfy boundary conditions at $z = 0$ and ∞. As for the free solutions discussed earlier, the physically relevant complementary function is $A\exp(\mathrm{i}\nu z - z/2H_0)$ which is consistent with upward energy propagation; A remains to be determined by the lower boundary condition as shown below. We shall require that the vertical velocity vanishes at the plane horizontal surface at $z = 0$ (representing the ground). Again this condition can be enforced through the linearized form of the thermodynamic equation (4), i.e.

$$U\frac{\partial^2}{\partial x \partial z}\left(\frac{\delta p}{\rho_0}\right) + N^2 w = gS. \quad \ldots\ \ldots\ \ldots\ \ldots\ \ldots\ \ldots\ (21)$$

The lower boundary condition is then

$$U\frac{\partial^2}{\partial x \partial z}\left(\frac{\delta p}{\rho_0}\right)\Big|_{z=0} = -\mathrm{i}ag\exp(\mathrm{i}kx)\cos\mu y$$

which can be shown, using equation (20) and the expression for C, to imply that

$$A = \frac{\frac{\rho_s a g}{Uk}\left(\mathrm{i}\nu - \frac{1}{2H_0}\right)}{b\gamma + \nu^2 + \frac{1}{4H_0^2}}$$

In deriving this expression, the dispersion relation equation (8), with $c = 0$, has been used. The full solution is therefore given by

$$\delta p = \mathrm{Re}\left[\frac{\frac{\rho_s a g}{Uk}\cos \mu y}{b\gamma + \nu^2 + \frac{1}{4H_0^2}} \left[\gamma \exp(-\gamma z) + \left(\mathrm{i}\nu - \frac{1}{2H_0}\right) \exp\left\{\left(\mathrm{i}\nu - \frac{1}{2H_0}\right) z\right\} \exp(\mathrm{i}kx)\right]\right] \tag{22}$$

where

$$\nu^2 = \left(\frac{N}{f_0}\right)^2 \left\{\frac{\beta}{U} - (k^2 + \mu^2)\right\} - \frac{1}{4H_0^2}$$

Notice that if the Charney/Drazin condition given by equation (9) is not satisfied, ν is imaginary and the disturbance energy decays with height. Equation (22) also implies that the response is inversely proportional to the basic state wind speed U. This is because air parcels spend a time proportional to $1/U$ in, say, the heating region of S and so the longer the time they spend there, the bigger the response. Fig. 5 shows some typical amplitude and phase plots of the geopotential height and temperature for wave numbers 1, 2 and 3 derived from equation (22) taking $a = 3$ K day^{-1}/260 K, $k = 2\pi m/30\,000$ km (where m is the wave number), $b = 1/(4$ km), $U = 10$ m s^{-1}, $B = 3 \times 10^{-5}$ m^{-1}, and μ chosen to correspond to a disturbance with one amplitude maximum in middle latitudes tending to zero at the pole and equator. Note that the geopotential height amplitude is given by $\delta p/\rho_0 g$. In Fig. 5 the phase of the wave ridge is plotted in trigonometrical degrees and not degrees longitude. However, for wave number 1 these coincide to within an arbitrary constant.

Characteristic features of these energy radiating solutions are:

(a) a strong surface pressure response (about 10 mb),
(b) mid-troposphere minimum amplitude (at about 3 or 4 km),
(c) wind amplitude increase at $\exp(z/2H_0)$ as $z \to \infty$ (specific kinetic energy, $\frac{1}{2}\rho_0(u_g^2 + v_g^2) =$ constant),
(d) strong westward tilt with height particularly in the heating region, and
(e) cold anticyclones on the eastern sides of continental land masses.

Characteristic (e) occurs because the surface pressure maximum occurs about 50° downstream of the diabatic cooling rate maximum. For evanescent waves with $\nu^2 < 0$, this phase difference is 90° and the same general conclusion holds. The diabatic cooling rate maximum is assumed to be central to the land mass and so the high pressure will occur to the east.

Waves which tilt to the west with height and which are geostrophically and hydrostatically balanced, transport heat polewards in the sense that $\overline{v_g\theta} > 0$ where the overbar denotes the zonal average. To show this, let the geopotential height perturbation associated with *any* wave field be given by

$$h = \frac{\delta p}{\rho_0 g} = H(z)\cos\{kx + \epsilon(z)\}$$

where $H(z)$ is the amplitude and $\epsilon(z)$ the phase. The hydrostatic equation can then be used to find θ' so that

$$\frac{\theta'}{\theta_0} = \frac{\partial h}{\partial z} = \frac{\mathrm{d}H}{\mathrm{d}z}\cos(kx + \epsilon) - H\sin(kx + \epsilon)\frac{\mathrm{d}\epsilon}{\mathrm{d}z}\,.$$

Also the geostrophic wind relation gives

$$v_g = \frac{g}{f}\frac{\partial h}{\partial x} = -\frac{g}{f}H(z)\,k\sin(kx + \epsilon)$$

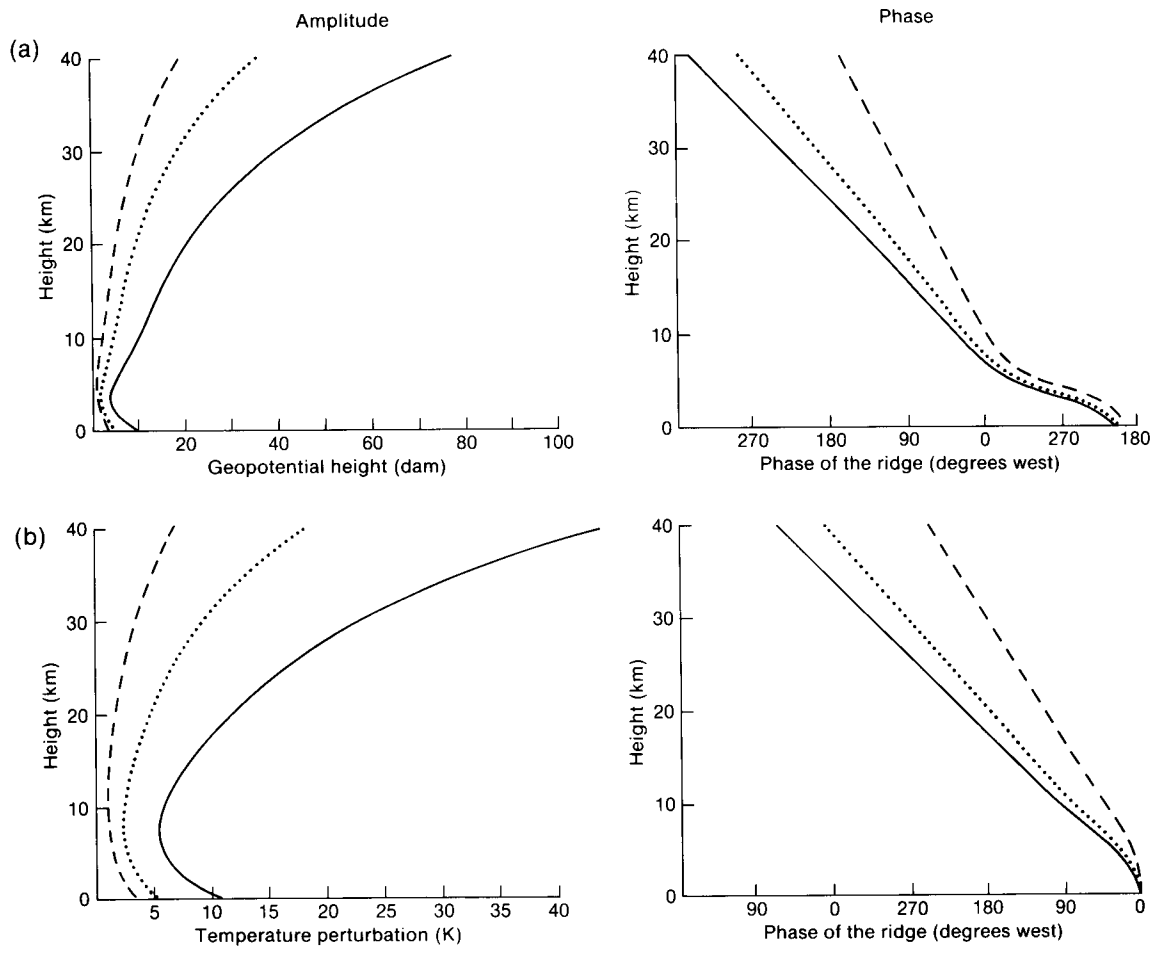

Figure 5. Amplitude and phase plots of (a) geopotential height and (b) temperature for wave numbers 1 (———), 2 (·····) and 3 (— — —) derived from equation (22).

so that

$$\overline{\theta' v_g} = \tfrac{1}{2}\, g\theta_0 \frac{k}{f} H^2 \frac{d\epsilon}{dz} .$$

Since westward phase tilt with height implies $d\epsilon/dz > 0$ then heat transport is poleward. Fig. 6 shows $\overline{v_g\theta}$ for wave number 1 derived from the analytic solution, equation (22). Above the heat source $\rho_0\overline{v_g\theta'}$ is independent of height. For reasons beyond the scope of this analysis one should be cautious before equating $\rho_0\overline{v_g\theta'}$ to any real tendency of stationary waves to transport heat. In the adiabatic regions of the model flow, parcels return from high latitudes with the same potential temperature as they set out with so that no real transport is achieved. This is not true of parcels in the lower tropospheric heating region which experience heating (on average) as they travel poleward and cooling as they travel equatorward, thereby achieving real heat transport.

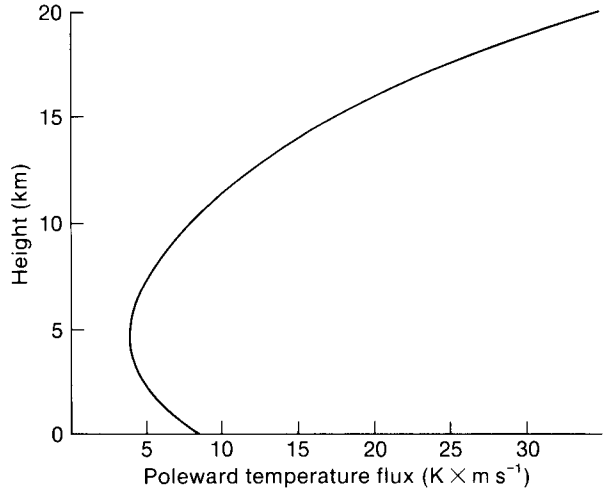

Figure 6. Height variation of poleward heat flux associated with the solution given by equation (20) for wave number 1.

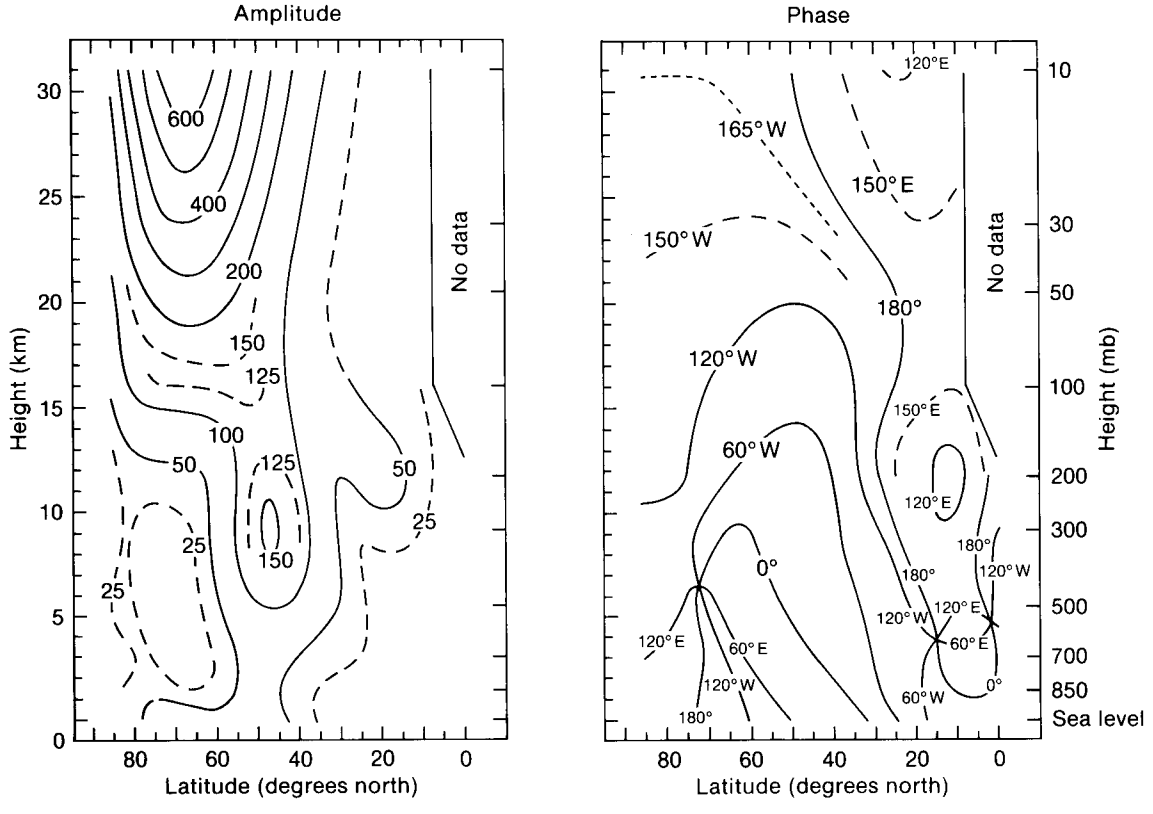

Figure 7. Long-term mean amplitude (m) and phase (degrees longitude) for the northern hemisphere in January for wave number 1, plotted as a function of height and latitude (van Loon *et al.* 1973).

6. Comparison with observations

Fig. 7 shows the observed, time-averaged winter-time amplitude and phase of wave number 1 as a function of height and latitude (from van Loon *et al.* 1973). There are many interesting points of agreement with the highly idealized solutions presented here including rapid phase tilt westward with height, amplification with height, and even the suggestion of an amplitude minimum near 3 km. Observations of the amplitude of wave numbers 1 and 2 up to a height of 100 km have been collated by Green (1972) and plotted on a logarithmic scale (Fig. 8(a)). The specific kinetic energy is found to be approximately constant with height up to 40 or 50 km, above which it falls off rapidly. The accompanying phase diagram (Fig. 8(b)) shows rapid phase tilt westward with height.

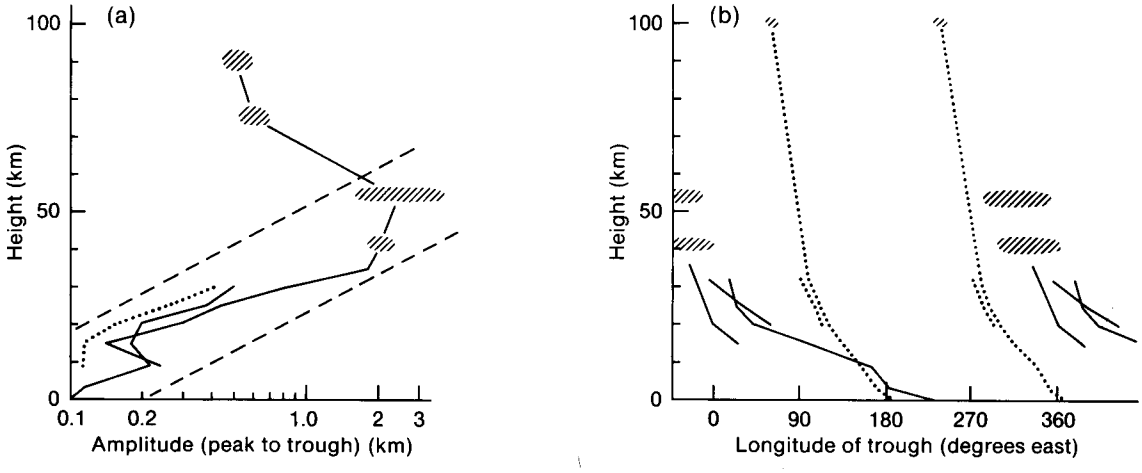

Figure 8. Observed variation with height of (a) geopotential height amplitude (plotted on a logarithmic scale) and (b) phase of the January mean eddy motion at 50° N for wave numbers 1 (———) and 2 (·····). Where the specific kinetic energy in (a) is constant with height the curve is parallel to the dashed lines. The shaded areas indicate the uncertainty inherent in the middle atmosphere data. For origin of data see Green (1972).

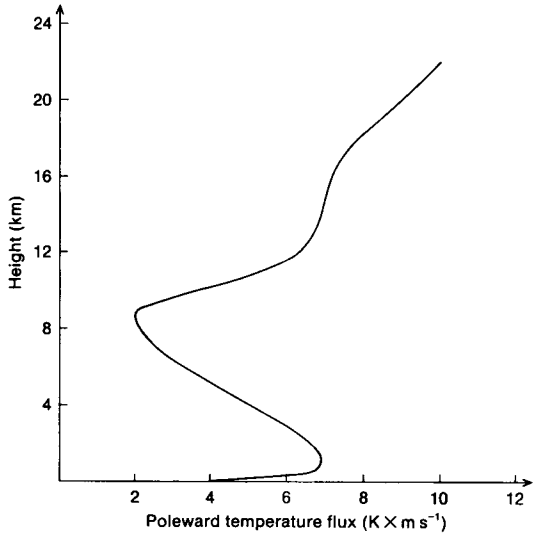

Figure 9. Vertical variation of the latitudinally-averaged poleward temperature flux caused by stationary waves for January 1963 (Shutts 1978).

The linear solution, equation (22), must break down at some height since the pressure perturbation amplitude falls off as exp $(-z/2H_0)$, compared to exp $(-z/H_0)$ for the basic state pressure, so that at some height the total pressure would become negative. In practice wave breakdown occurs long before this as a non-linear advection process. The absorption of disturbance energy in the stratosphere through the breakdown process is probably the dominant mechanism for the tail-off of the specific kinetic energy.

Fig. 9 shows the observed poleward heat transport due to stationary waves in January 1963. The low-level maximum and 'whip-lash' amplification effect in the stratosphere are both in agreement with the model heat flux portrayed in Fig. 6. Since the stationary wave heat transport (primarily wave numbers 1, 2 and 3) constitutes about 50% of the total atmospheric poleward heat transport in winter, vertically propagating ultra-long waves probably play an important role in the global heat budget. Further solutions for more realistic distributions of N^2 and U (with height) can be found in Shutts (1978).

References

Charney, J.G. and Drazin, P.G. 1961 Propagation of planetary-scale disturbances from the lower into the upper atmosphere. *J Geophys Res*, **66**, 83–109.

Gill, A.E. 1982 Atmosphere-ocean dynamics. London, Academic Press, International Geophysics Series, Vol. 30.

Green, J.S.A. 1972 Large-scale motion in the upper stratosphere and mesosphere: an evaluation of data and theories. *Philos Trans R Soc London*, A, **271**, 577–583.

Lau, N–C. 1979 The observed structure of tropospheric stationary waves and the local balances of vorticity and heat. *J Atmos Sci*, **36**, 996–1016.

Shutts, G.J. 1978 Quasi-geostrophic planetary wave forcing. *Q J R Meteorol Soc*, **104**, 331–350.

van Loon, H., Jenne, R.L. and Labitzke, K. 1973 Zonal harmonic standing waves. *J Geophys Res*, **78**, 4463–4471.

551.553.6(427)

An analysis of wind speed and direction at a high-altitude site in the southern Pennines

P.A. Smithson

University of Sheffield

Summary

An analysis is presented of hourly wind data from High Bradfield, a high-altitude (405 m) anemograph site in the southern Pennines, based on the period 1975–84. Comparison is made with other UK sites to assess the distinctive properties of airflow at this site. Mean values, extremes, return periods and gale frequencies are examined.

1. Introduction

The wind climatology of the British Isles, based on a scattered distribution of anemographs, has been described by Shellard (1976) and its application to building design has been surveyed by Lacy (1977). A number of locations have been examined in detail, e.g. Sheffield (Lee 1975) and Ballykelly (Glassey and Durbin 1971). Hardman *et al.* (1973) and Caton (1976) have also produced generalized maps of extreme

wind speeds and hourly mean wind speeds respectively by interpolating between the rather sparse network of anemometer sites. However, few anemometers are located in upland areas, so the results over high ground may not be very reliable. Barry (1981) states that the most important characteristics of wind velocity over mountains are related to topography rather than altitude. It is unlikely, therefore, that the wind characteristics of an upland site could be predicted fully by extrapolating or modelling based on lowland data alone.

An anemometer has been operational at High Bradfield, South Yorkshire since November 1974. Its vane-level altitude is 405 m and it is the most southerly high-level anemograph site in the United Kingdom. The other three sites above 400 m published in the *Monthly Weather Report* are in Scotland (Lowther Hill, 754 m), the Isle of Man (Snaefell, 628 m) and the northern Pennines (Great Dun Fell, 857 m). No detailed analyses appear to have been published for any of these sites, though brief notes about Cairn Gorm automatic weather station (1245 m) have appeared (Curran *et al.* 1977 and Barton 1981). Wind observations were taken on Ben Nevis (1343 m) from 1883 to 1904 but were based on a relative, rather than an absolute, scale which makes their use difficult. With over 10 years' data being available, the High Bradfield record is now sufficiently long to draw some general conclusions about the nature of airflow at high levels in the southern Pennines.

2. Site details

The anemometer at High Bradfield is sited on the flat summit of a ridge extending in an approximately west to east direction on the eastern slopes of the Pennines, 7.5 km north-west of the University of Sheffield's anemometer (Fig. 1). To the south-west, the Loxley valley has incised deeply into the foothills of the Pennines, generating a tendency for funnelling in the valley with winds from

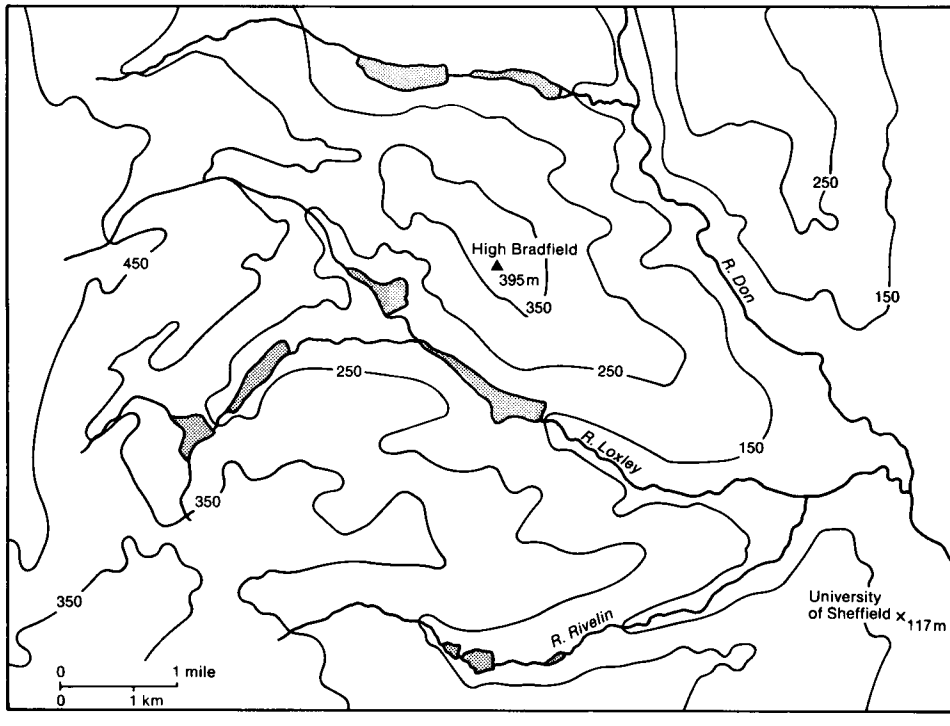

Figure 1. Map of the area around the High Bradfield site with heights shown in metres and reservoirs stippled.

between north-west and south-west. In general the site (with an effective anemometer height of 10 m) is fully exposed in all directions apart from minor turbulence produced by low buildings and walls in the vicinity. There has been no change of location during the period of operation. A number of minor interruptions to the record have occurred due to instrumental faults or severe weather when icing or rime has affected the operation of the cups or vane. No more than 4.7% of the total speed record was missing. The direction trace was a little more erratic with about 11% of the record missing; September had the highest incidence of non-operation. Although this figure may appear high compared with lowland sites, defective records are much more frequent at higher altitudes.

The data are in the form of hourly mean wind speeds and directions, speeds of the maximum gust for each hour and for the daily maximum gusts; directions of the gusts are also available. For the 10-year period 1975–84, a total of over 83 000 hourly values have been analysed. Manual extraction of data for the subsequent period was possible and used in sections 3.3, 4 and 5 to increase the sample size, but did not form part of the computer analysis in sections 3.1 and 3.2.

3. Mean speeds

3.1 *Monthly variation of mean speed*

Table I shows the monthly variations of hourly mean wind speeds at High Bradfield. A seasonal pattern is evident with the highest value in January and the lowest in August; there is also a secondary peak in March. An interesting feature is that the values for February and October are somewhat less than might be expected from adjacent monthly values; an identical result to that found by Smith (1984) at Elmdon (Birmingham Airport) for the period 1965–79. Smith argued that these anomalies were almost certainly caused by sampling inadequacies because a more regular change throughout the year was obtained when using pressure values as surrogate measures of wind speed for a 100-year period (Smith 1983). Nevertheless, it is surprising that a similar pattern to that at Elmdon was found despite the differences in altitude, physical separation and only a 5-year overlap in the time periods. Presumably Februarys and Octobers of the 1965–84 period have been less windy than formerly, perhaps associated with more frequent blocking in February and the warming which has taken place in October (Clarke 1966, Wright 1976).

Table I. *Means and standard deviations of hourly wind speeds (kn) at High Bradfield, 1975–84*

	Mean	Standard deviation	Sample size
Jan.	18.7	11.2	7 411
Feb.	13.4	8.4	6 439
Mar.	15.9	9.1	7 069
Apr.	13.1	7.6	7 000
May	11.4	6.1	7 135
June	11.9	6.4	6 966
July	11.2	6.0	6 963
Aug.	10.6	6.3	7 062
Sept.	14.8	8.1	6 506
Oct.	14.7	8.6	6 981
Nov.	17.0	9.7	6 945
Dec.	16.5	9.6	7 061
Year	14.1	8.6	83 538

Seasonal differences in mean speed at High Bradfield are large in contrast to more lowland sites. Using the average values of mean wind speed for 1961–70 at sites listed in Shellard (1976), the ratios of the windiest month to the least windy month range from 1.81 for the Isles of Scilly to 1.21 at Elmdon. High ratios tend to be at coastal sites and low ratios at inland sites. The seasonal ratios do suggest that high-altitude sites, as exemplified by High Bradfield, have a similar seasonal pattern of wind speeds to those of the most exposed coastal locations on the west and south coasts. However, the ratio does tend to vary depending upon the time period examined. At Great Dun Fell, the highest anemometer site for which long-period records are available, the ratio for the period 1974–84 is 1.67 which is similar to that of High Bradfield for a similar period, but for the period 1964–84 the ratio drops to 1.40. It would appear that a 10-year period may be too short to provide an adequate assessment of the ratio of winter to summer monthly mean wind speed. However, some sites, e.g. Heathrow and the Isles of Scilly, do show similar ratios from 1961–70 to 1971–80. Unfortunately there are insufficient long-period anemograph sites at high altitudes to test this similarity with exposed coastal locations in the south and west.

Instead of using the absolute values, it is possible to examine the seasonal variation in wind speed by calculating a standardized anomaly for each monthly mean speed, i.e. expressing each monthly value as the deviation from the annual mean divided by the standard deviation of the monthly speeds. Smith (1983) used this method to distinguish between lowland locations in the west and extreme north of the United Kingdom and all other lowland sites. The mean standardized anomalies for the two areas obtained by Smith are plotted in Fig. 2 together with the equivalent values for High Bradfield (1975–84) and Great Dun Fell (1964–84). A similar pattern is exhibited by all sites, but the two high-altitude sites emphasize the difference noted by Smith, i.e. for the western and extreme northern areas, the standardized anomalies tend to be weaker than for the area further south and east in the spring but stronger in autumn and early winter.

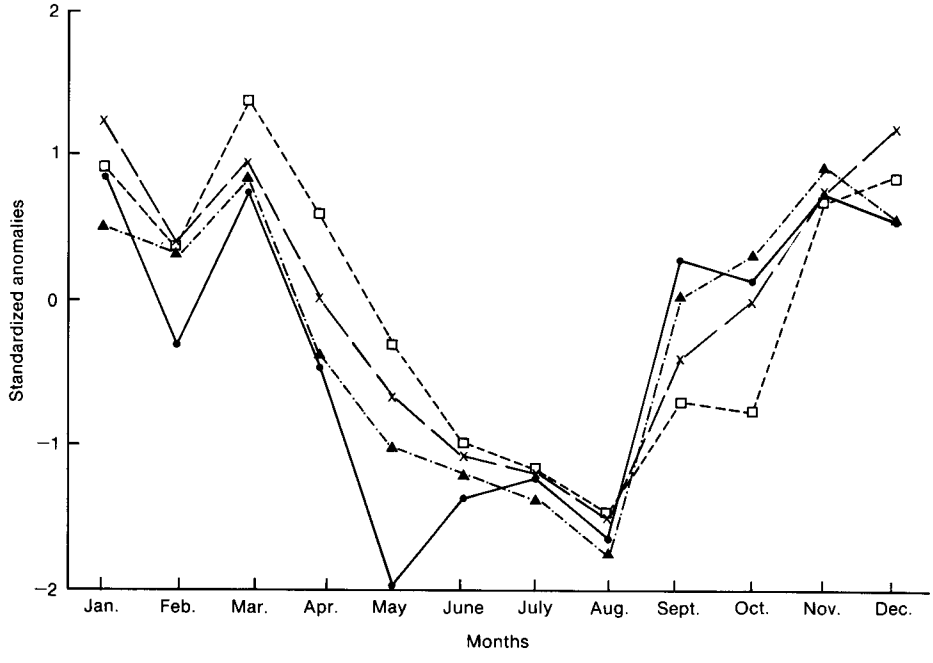

Figure 2. Mean standardized anomalies of monthly wind speeds for western and extreme northern sites of the United Kingdom (×——×) and all other lowland locations (□- -□) (after Smith 1983), High Bradfield (1975–84) (•——•) and Great Dun Fell (1964–84) (▲ ·—·▲).

3.2 *Cumulative frequency*

The use of mean values of wind speed is not always justified because wind speed does not have a statistically normal distribution. Work on wind speed distribution in the United Kingdom indicates that, for speeds greater than about 10 knots, the Weibull distribution is a good approximation to the cumulative frequency pattern (Caton 1976). For each month of the 10-year period, frequencies of hourly mean wind speeds at High Bradfield were obtained for the standard speed classes listed in published work, viz. 1–3, 4–6, 7–10, 11–16, 17–21, 22–27, 28–33, 34–40, 41–47, 48–55, 56–63, and >63 knots. From the cumulative percentage frequencies the Weibull distribution parameters were derived and estimates made of the speed which would be exceeded for specified proportions of time (Tackle and Brown 1978). Table II lists the wind speeds in knots for each month of the year which would be exceeded for 75%, 50%, 25%, 10%, 5%, 1% and 0.1% of the time. For each category the ranking of monthly speeds is similar to that given by the monthly mean figures. Points worthy of note are that August, whilst having the lowest speeds for the majority of the time, is prone occasionally to much stronger winds; this is supported by the nature of 1985 (outside the period of the analysis) when 37 hours on 8 days had hourly mean wind speeds above 29 knots, the 1% value. July demonstrates the reverse pattern with fewer strong winds than would be expected from its mean speed. Although October appears anomalous by exhibiting a decline in mean wind speed relative to September, there is little difference between the two months on the basis of the Weibull distribution. January stands out as the windiest month in the period studied; it has a slightly higher frequency of low speeds than November but this is more than compensated for by its greater frequency of high speeds.

Table II. *Wind speeds (kn) likely to be exceeded by a given percentage of the time at High Bradfield, 1975–84, based on the Weibull distribution*

	Percentage of time						
	75	50	25	10	5	1	0.1
Jan.	8.7	16.1	24.1	32.8	38.4	48.9	62.1
Feb.	6.8	11.4	17.5	23.7	28.3	36.9	46.6
Mar.	8.3	13.6	20.2	27.4	31.6	40.7	50.8
Apr.	6.6	11.1	16.7	22.9	27.0	34.9	44.2
May	6.2	10.1	14.6	19.2	22.5	28.3	34.9
June	6.8	10.5	14.9	19.6	22.9	28.9	34.9
July	6.4	10.1	14.6	19.2	22.1	27.5	34.5
Aug.	5.6	9.3	14.2	19.0	22.9	29.3	37.2
Sept.	8.1	13.2	19.4	25.8	30.5	38.6	48.1
Oct.	7.8	12.8	19.0	26.0	30.5	38.8	48.9
Nov.	9.3	14.7	21.5	28.7	33.0	40.9	50.8
Dec.	8.9	14.6	21.7	29.1	34.3	43.1	54.3

Caton (1976), in his study of hourly mean wind speeds over the United Kingdom for the period 1965–73, mapped the speeds likely to be exceeded for various percentages of time for sites between mean sea level and an altitude of 70 m after local effects had been eliminated. Where a site exceeded 70 m in altitude, a correction factor to the mapped value was recommended. The 75 and 50 percentile values were to be increased by 7%, the 25, 10 and 5 percentile values by 8% and the 1 and 0.1 percentile values by 9% per 100 m of height above the plain or above the 70 m contour as appropriate. It was stressed that these corrections were very tentative, particularly above 400 m. Although based on a different time period, the High Bradfield data have been analysed in a similar manner to that used by Caton, so should provide an interesting check on Caton's correction factors. The lowland wind speed value at the location of High Bradfield was extracted from the maps, adjusted by the altitudinal correction factor suggested

by Caton, and then converted to knots for comparison with the remaining data (Table III). As can be seen, the predicted hourly mean wind speeds are consistently less than those for High Bradfield by about 20%. To give a good estimate of the actual values, the lowland speeds should have a correction factor of about double that used by Caton, i.e. 14% for the 75 and 50 percentiles, 16% for the 25 and 10 percentiles and 18% per 100 m for the 5, 1 and 0.1 percentiles. It should not be forgotten that Caton's work was based on a different period from that at High Bradfield.

Confirmation of the validity of the higher correction factor for speeds at heights above 400 m is indicated by the Great Dun Fell data. Taking the 50% value for lowland speeds at the site of Great Dun Fell, and applying the 14% per 100 m above 70 m altitude correction factor, gives a mean speed only slightly below that for 1964–84.

Table III. *Comparison of observed wind speeds (kn) for High Bradfield, 1975–84 with values predicted by Caton's (1976) method, based on the Weibull distribution as in Table II.*

		Percentage of time						
		75	50	25	10	5	1	0.1
Observed	(a)	7.2	12.0	18.4	25.0	29.3	38.0	48.1
Caton (lowland)	(b)	4.9	8.0	11.6	15.5	17.8	23.5	31.2
Caton (for 405 m)	(c)	6.1	9.9	14.7	19.7	22.6	30.6	40.6
(c)/(a) (per cent)		85	83	80	79	77	81	84

3.3 *Extreme values*

The series of annual maximum hourly speeds was analysed using standard statistical methods of extreme values (Gumbel 1958). The maximum value likely to be exceeded only once in T years can then be calculated. This approach was taken by Hardman *et al.* (1973) for 144 stations over the United Kingdom in order to map the isopleths of once in 50-year hourly mean wind speeds and gust speeds over open country. Attempts were also made to predict extreme winds on exposed hilltops on the basis of nearby (but lower) stations using a power law with exponent 0.17. For gust speeds, the power-law expression provided estimates which were lower than the value obtained from the original record but the application of a gust factor of 1.4 to the hourly mean wind speeds gave estimates which were comparable. Estimates of the maximum hourly mean wind speeds for given return periods are listed in Table IV. Inevitably the computed extremes should be treated with caution as the error terms in the prediction are high. However, they do provide a guide to the magnitude of extreme winds likely to be experienced at high-altitude sites in the United Kingdom.

Table IV. *Maximum hourly mean wind speeds and gusts (kn) for given return periods at High Bradfield, (1975–85)*

Hourly mean wind speeds Return period (years)						Gust speeds Return period (years)					
Mean	10	20	50	100	120	Mean	10	20	50	100	120
59	68	72	76	80	81	84	99	106	114	120	121

4. Maximum gusts

Hourly mean wind speed provides a good measure of wind strength at a site but of equal importance is the instantaneous strength of wind to which individuals or buildings may be exposed. It is these gusts of wind which are responsible for much of the damage which occurs during stormy weather and hence are of considerable practical importance. Table V lists the mean monthly maximum gust for the period December 1974 to June 1986 at High Bradfield together with the highest gust recorded. A similar pattern of ranking to that given by the mean speeds is obtained, with January as the month with the highest gusts and July with the lowest. As expected, the period from April to August has the lowest mean maximum gusts together with relatively low variability as indicated by the standard deviations. In winter, not only are the gusts stronger on average but also there is a greater inter-annual variability.

Table V. *Maximum gust data (kn) for High Bradfield based on monthly values from December 1974 to June 1986*

	Mean monthly maximum gust	Standard deviation	Maximum gust	Year of occurrence
Jan.	76.4	11.9	99	1984
Feb.	57.3	13.9	82	1983
Mar.	63.6	9.0	74	1978
Apr.	55.8	9.5	68	1985
May	50.0	8.1	64	1982
June	49.1	6.9	62	1983
July	45.8	4.6	52	1977
Aug.	48.4	9.6	63	1985
Sept.	64.5	11.5	84	1975
Oct.	62.0	7.4	72	1981, 83
Nov.	68.9	11.5	94	1980
Dec.	70.9	15.6	99	1974

In addition to considering only the highest gust for each month, the data enable the maximum gust for each hour to be analysed though its significance will be less than the monthly maxima referred to earlier. For more than half the year, between September and March inclusive, hourly maximum gusts are likely to exceed 20 knots for 50% of the time (Table VI). During the period studied, only February did not achieve this level. Earlier discussion about anomalies in the seasonal pattern caused by short-period sampling would indicate that the lower value for February is a sampling problem rather than a real feature of the climate. A value of 0.1% of the time represents seven occurrences in 10 years with hourly maximum gusts reaching or exceeding the given speed. Examination of the actual frequency of occurrence for the period 1975–84 indicates that the Weibull distribution slightly underestimates the frequency for the five months which had seven occurrences or less of the 0.1% speed. May and August recorded 23 occasions of hourly maximum gusts above the 0.1% value.

Estimates of the gust speeds for specified return periods are given in Table IV using the same method as Hardman *et al.* (1973); gusts of over 100 knots would be expected at least once in 10 years. The gust factor based on hourly values averages 1.64 with only slight variability throughout the year. This is in accordance with its exposed and relatively unobstructed situation and only slightly above the figure of 1.6 quoted by Shellard (1976) for the gust factor over more or less flat country with few obstructions. The effect of altitude on this wind property would appear to be of less importance than local factors.

Table VI. *Maximum hourly gust speeds (kn) likely to be exceeded by a given percentage of the time at High Bradfield from December 1974 to June 1986, based on the Weibull distribution*

	Percentage of time						
	75	50	25	10	5	1	0.1
Jan.	16.1	25.4	37.2	49.9	57.4	71.8	88.9
Feb.	10.9	17.8	27.0	35.9	42.3	53.9	67.9
Mar.	14.4	22.5	32.0	41.1	46.8	58.2	71.4
Apr.	11.8	18.6	27.2	35.5	40.7	50.8	62.0
May	10.9	16.5	23.1	29.3	33.4	40.7	49.3
June	11.6	17.7	24.8	31.6	36.1	44.4	53.5
July	10.7	16.5	23.3	29.9	34.1	42.1	50.8
Aug.	9.5	15.1	22.3	29.5	34.1	42.7	52.4
Sept.	14.0	21.5	30.5	38.8	44.6	54.3	65.6
Oct.	13.2	20.8	29.9	39.2	45.0	53.9	68.3
Nov.	15.3	23.9	33.6	43.1	49.5	60.5	73.7
Dec.	14.9	23.5	34.1	45.0	52.0	64.4	79.5
Year	11.3	18.6	28.9	39.4	46.0	58.6	73.9

5. Gales

Gale frequencies are often quoted as a measure of the windiness of a site. A day of gale is defined as a day on which the wind speed at the standard height of 10 metres attains a mean value of 34 knots or more over any period of ten consecutive minutes during the day (Meteorological Office 1972). The data at High Bradfield are not easily related to this definition as only hourly mean wind speeds and hourly maximum gusts are recorded. Two alternative definitions could be used. The more rigorous one would be for a day of gale to experience a speed of at least 34 knots for a period of one hour. A second definition could be, a day on which at least one gust reached 34 knots or more. As the latter definition is not normally applied, only data satisfying the former definition are analysed.

Breaks in the record make it impossible to give a precise total of the number of hours between December 1974 and June 1986 which experienced an hourly mean wind speed above 33 knots, though on occasion some interpolation was possible. For short interruptions, weather maps could be examined and comparison made with the nearby anemograph at Sheffield to check if any hours were likely to have reached the critical mean speed. For longer breaks no interpolation was possible. To reduce the impact of interruptions in the record, Table VII gives the proportion of the available record that hourly mean wind speeds were equal to or above the critical values rather than monthly average figures.

Year-to-year variability characterizes the record; some years are very windy whilst others are relatively calm. All months except January and December experienced at least one occurrence with no hourly mean wind speed above 33 knots. At the other extreme, more than 35% of all hours in December 1974 had a mean speed above gale force, a factor no doubt important in making it the second mildest December in the last hundred years over England and Wales. The ranking of the number of hours with gales does conform closely to the mean speed rank, though August contains more gales than its mean speed suggests whilst June and September have fewer gales. The value for September could be anomalous as only seven months had complete records and two with incomplete records had already received more than the average value. For severe gales with hourly mean wind speeds of at least 48 knots, January and December became the only months with a significant number of hours and even in these months some years did not attain this speed. From April to August inclusive, hourly mean wind speeds of at least 48 knots are very unlikely.

Table VII. *Frequency and percentage data of occasions when hourly mean wind speeds exceeded given values (kn) for High Bradfield from December 1974 to June 1986*

	No. of hours ≥34	Range* in no. of hours	Percentage of record ≥34	No. of hours ≥48	Range* in no. of hours	Percentage of record ≥48
Jan.	912	11–192	10.3	142	0–56	1.6
Feb.	172	0–60	2.1	11	0–7	0.2
Mar.	413	0–99	5.2	16	0–7	0.2
Apr.	140	0–66	1.7	2	0–1	0.02
May	63	0–11	0.7			
June	18	0–7	0.2			
July	10	0–8	0.1			
Aug.	37	0–14	0.5			
Sept.	144	0–30	2.0	12	0–4	0.1
Oct.	267	0–66	3.4	4	0–2	0.05
Nov.	482	0–115	6.3	13	0–4	0.2
Dec.	794	3–265	9.3	65	0–30	0.8

* Lower value of range for complete months only.

6. Diurnal variations

The diurnal variation of wind speed at inland locations is usually well marked with a maximum in the early afternoon and a minimum shortly before sunrise, the actual times and the amplitude of the average variation depending upon the time of year (Shellard 1976). The upland location of High Bradfield would suggest that diurnal heating and therefore the amplitude of the diurnal wind speed would be less than that at lowland sites. At Kew, the diurnal amplitude for June–August was 4.5 knots for the period 1959–68 compared with only 2.2 knots for December–February despite the higher mean speed. At High Bradfield, the mean diurnal variation for the same two periods was only 2.5 knots and 1.2 knots respectively; this supports the belief that the diurnal amplitude would be less at higher altitudes. For most months of the year, the highest mean speed occurs between 1100 and 1700 GMT. Only in February and November does it occur during night-time hours. With reduced solar heating at this time of year, the time of maximum mean speed is randomly distributed, especially in view of the limited diurnal range in these months. The difference between the highest and lowest hourly mean value was found to be non-significant at the 5% level using Student's *t*-test for the months from November to February whereas the difference was significant for the remaining months. For the year as a whole, the hours from 1200 to 1500 GMT have the highest mean speed at 15.1 knots and from 0400 to 0700 GMT have the lowest mean speed at 13.5 knots, a range of only 1.6 knots. Because of the large sample size, the difference in this instance was statistically significant at the 0.1% level.

7. Direction

Wind direction is less likely to be affected by altitude than wind speed. The reduced surface roughness and friction at hilltop sites should produce a slight veering of the wind relative to lower altitude sites so that the airflow more closely resembles the gradient wind. The annual pattern (Fig. 3) shows the prevailing direction to be from 230° to 250°, with a secondary and minor maximum from 020° to 040°. Winds between 080° and 160° are infrequent and calms and variable winds unusual. The annual figures mask monthly variations in wind direction which reflect the seasonal cycle of pressure patterns and depression tracks throughout the year (Perry 1976). The main features of the seasonal pattern (Fig. 4) are the dominance of westerly sector winds from September to January, and a higher frequency of

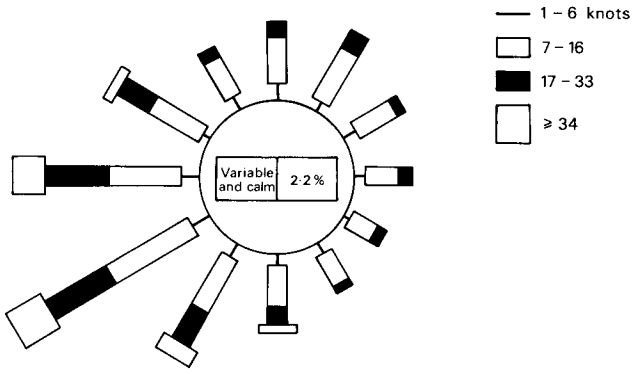

Figure 3. Annual wind rose of hourly means for High Bradfield.

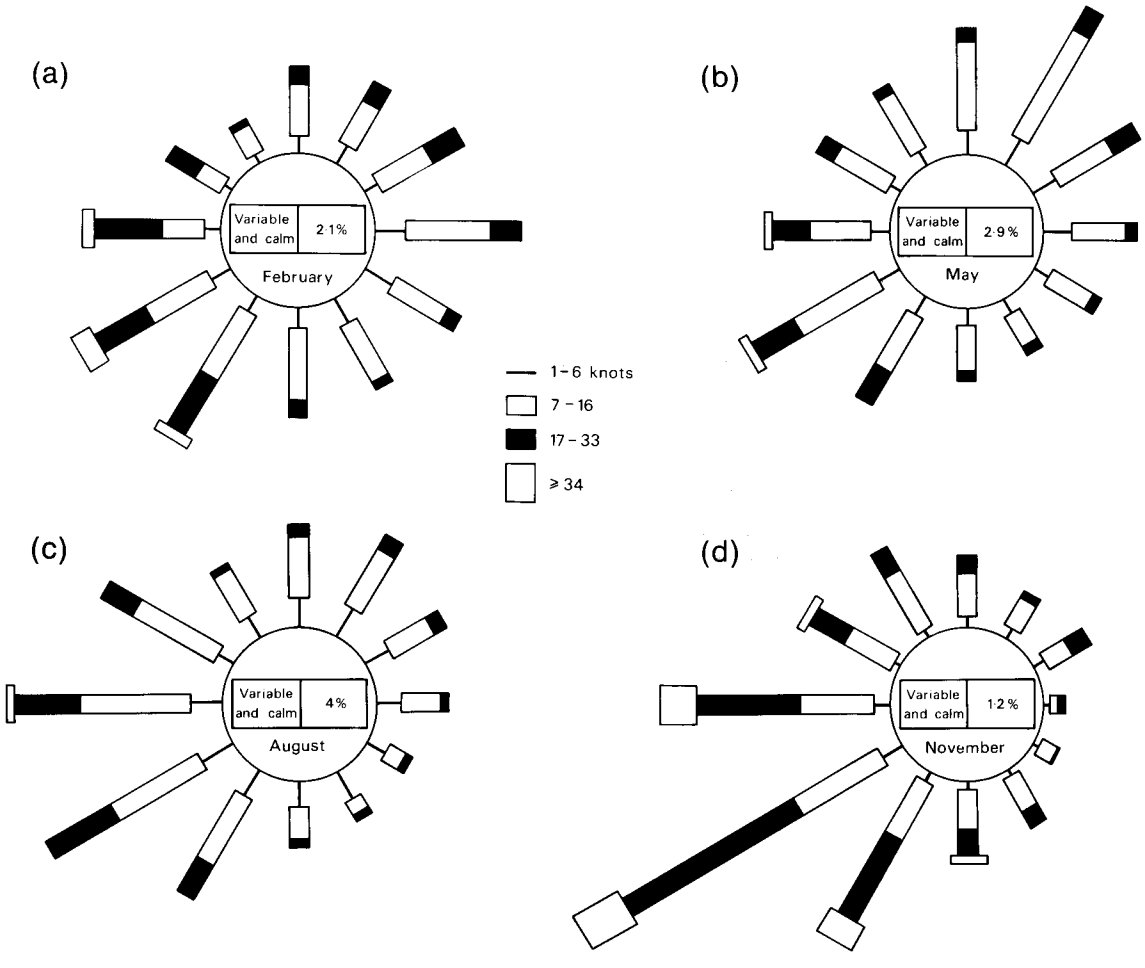

Figure 4. Wind roses of hourly means for (a) February, (b) May, (c) August and (d) November for High Bradfield.

easterly winds in February and northerly sector winds from March to May when westerlies reach their lowest proportion, a frequently noted aspect of our climate. The distribution for the summer months is similar to the annual pattern though there is a reduced dominance of westerlies in August. Winds between 170° and 220° are most common in autumn. In general the directional properties of airflow at High Bradfield do not differ markedly from those at lower altitudes. Local factors, such as sea-breezes or topography, which can be significant in affecting the wind rose on the coast or at low-altitude inland locations, do not appear to be important at this hilltop site.

The relationship between direction and speed reinforces the general dominance of westerly winds. Not only are winds most frequent from this direction but also the higher speeds are almost always between 200° and 280°. More than 75% of hourly mean winds greater than 33 knots blow from between 230° and 280° and more than 90% from between 200° and 280°. For the year as a whole, the 11–16 knot class represents the modal value for all directions. However, minor differences occur during the year, with a tendency for a lower modal value for northerlies and easterlies during the summer half-year and for a higher modal value for westerlies in the winter half-year.

8. Conclusions

The pattern of wind speeds over lowland United Kingdom has been well established (Hardman *et al.* 1973, Caton 1976, Shellard 1976) in terms of mean speeds and probabilities of extreme events. Few anemographs have operated above 150 m, so information about wind speed at higher altitudes has been limited. Short-period instrumentation or model predictions from lowland sites have been used to overcome the problem with some success but verification of the models from longer-period sites has been needed. The anemometer at High Bradfield has been in operation since 1974 and, although a proportion of records are missing, it provides an indication of the range of wind speeds which can be expected at only moderate altitudes in England. Gales are a frequent feature of its climate. Winter storms batter the area with westerly winds of severe-gale strength and even in summer, gales occur in most months although of more moderate intensity and duration than their winter counterparts. All sites possess an element of uniqueness derived from local factors of altitude, surface roughness and exposure. The open nature of the High Bradfield site should provide a satisfactory measure of hilltop airflow from which modifications at other sites could be generated by funnelling or shelter.

9. Acknowledgements

The author would like to thank the Meteorological Office for kindly providing the data on magnetic tape and R. Coleman of the Computer Services Unit, University of Sheffield for all her programming efforts.

References

Barry, R.G.	1981	Mountain weather and climate. London, Methuen.
Barton, J.S.	1981	Severe wind chill on Cairn Gorm. *Weather*, **36**, 313.
Caton, P.G.F.	1976	Maps of hourly mean wind speed over the United Kingdom 1965–73. *Climatol Mem, Meteorol Off*, No.79.
Clarke, P.C.	1966	Temperature and rainfall trends in October. *Weather*, **21**, 364–366.
Curran, J.C., Peckham, G.E., Smith, D., Thom, A.S., McCulloch, J.S.G. and Strangeways, I.C.	1977	Cairngorm summit automatic weather station. *Weather*, **32**, 61–63.
Glassey, S.D. and Durbin, W.G.	1971	Wind at Ballykelly. *Climatol Mem, Meteorol Off*, No. 68.
Gumbel, E.J.	1958	Statistics of extremes. New York, Columbia University Press.

Hardman, C.E., Helliwell, N.C. and Hopkins, J.S.	1973	Extreme wind speeds over the United Kingdom for periods ending 1971. *Climatol Mem, Meteorol Off*, No. 50A.
Lacy, R.E.	1977	Climate and building in Britain. Building Research Establishment report. London, HMSO.
Lee, B.E.	1975	The wind climate of Sheffield. Building Science Report No. 27, (Unpublished, copy available in the University of Sheffield.)
Meteorological Office	1972	Meteorological Glossary. London, HMSO.
Perry, A.H.	1976	Synoptic climatology. *In* Chandler, T.J. and Gregory, S. (eds); The Climate of the British Isles. London, Longman.
Shellard, H.C.	1976	Wind. *In* Chandler, T.J. and Gregory. S. (eds); The Climate of the British Isles. London, Longman.
Smith, S.G.	1983	Seasonal variation of wind speed in the United Kingdom. *Weather*, **38**, 98–103.
	1984	A stochastic model to generate sequences of hourly mean wind speeds for different sites in the United Kingdom. *J Climatol*, **4**, 133–148.
Tackle, E.S. and Brown, J.M.	1978	Note on the use of Weibull statistics to characterize wind-speed data. *J Appl Meteorol*, **17**, 556–559.
Wright, P.B.	1976	Recent climatic change. *In* Chandler, T.J. and Gregory, S. (eds); The Climate of the British Isles. London, Longman.

Correspondence

551.551.5

Comments on 'Prolonged clear air turbulence over the British Isles on 4 September 1985'

Dr Hisscott's article* on prolonged clear air turbulence over the British Isles has been read with interest, as it is not often that the same aircraft encounters turbulence over such a long period of time. Although he says that the turbulence covered a large area, was there any evidence to support the view that turbulence affected a large area vertically and laterally, other than longitudinally along the track?

The frontal zone shown on the Aberporth sounding for 0600 GMT on 4 September is at around 600 mb (14 000 ft approximately) which, with the surface warm front near south-west Ireland at 0600 GMT, gives an average frontal slope of 1:135. Moving this frontal slope at the speed of the surface warm front (north-east at about 27 kn) would put the frontal zone on the 0600 GMT sounding very near to the flight path both vertically and longitudinally at 0800–0900 GMT; indeed the pilot mentioned that they were flying just below the (pre-frontal) thick layer cloud. By 1000–1100 GMT (assuming no changes of frontal speed or slope) the frontal zone and thick cloud would have lowered some 4000 ft — to the new flight level of 10 000 ft!

On the 0600 GMT Aberporth sounding there is a vertical wind shear of 16 kn between 600 mb and 623 mb (a height difference of about 1000 ft) giving a shear of 16 kn/1000 ft (neglecting the small wind direction change with height). In aviation forecasting a vertical wind shear of over 6 kn/1000 ft is taken to be a condition suitable for moderate turbulence, and a vertical wind shear of over 10 kn/1000 ft to be a condition for severe turbulence. A vertical wind shear of over 15 kn/1000 ft is in my experience a rare event, which I have occasionally seen on ascents from Atlantic weather ships and Europe, usually underneath (i.e. below 18 000 ft) or above (i.e. above 40 000 ft) the polar front jet streams. Shears in

*Hisscott, L.A.; Prolonged clear air turbulence over the British Isles on 4 September 1985, *Meteorol Mag*, **115**, 1986, 329–331.

excess of 10 kn/1000 ft can often be followed over 06–24 hour intervals in the relatively dense upper-air network over Europe, together with reports of associated turbulence.

The two most potent mechanisms responsible for clear air turbulence are vertical and horizontal shears, and waves in the lee of a mountain barrier (see, for example, WMO Technical Note No 155, 1977). It is very likely that on this occasion there was sufficient vertical shear present to account for the turbulence, neglecting any effect of the less easily measured horizontal shear and the effect of a wind in excess of 20 kn blowing in a stable airstream over the Welsh mountains. The decision to fly lower on the return leg, presumably in order to stay in clear air under the frontal cloud sheet, may have put the aircraft in the same zone of strong vertical shear as on the outward leg.

Although it was stated in the article that the turbulence was associated with the diffluence and anticyclonic turning below the warm frontal zone, it is hard to visualize physically this effect producing turbulence of that intensity and duration, considering that the winds in the lower troposphere were not all that strong, that there was little change in pattern shape, and that there was comparatively little change in the degree of turning. The jet stream of about 135 kn at around 35 800 ft from central Ireland to Cumbria to Norfolk at 0600 GMT may well have produced some turbulence due to diffluence, anticyclonic turning and wind shears, accounting for the SIGMET issued, but I would suggest that the prolonged and moderate to occasionally severe turbulence on that occasion was primarily due to flying in a shallow zone of very strong vertical wind shear under the frontal zone as it moved north-east and lowered, perhaps complicated by the fact that there was a dry adiabatic lapse rate between 700 mb (10 000 ft) and 623 mb (≈ 12 800 ft).

D.J. George

Regional Area Forecast Centre
Bracknell, Berkshire

551.551.5

Reply by L.A. Hisscott

As Mr George suggests, it is likely that the aircraft was flying in a similar position relative to the frontal zone on both sectors, and the strong vertical wind shear under the frontal zone is the probable cause of this phenomenon. Assuming that the conditions were not orographically induced, the warm front moving approximately perpendicular to the track at around 27 kn for the duration of the reported clear air turbulence would suggest a lateral extent of at least 80 n mile. The dry adiabatic lapse rate in the layer below the frontal zone may have pre-existed or been generated by the wind-shear induced turbulence, but in either case turbulent momentum transfer within the layer would probably distribute the disturbance vertically, perhaps so assisting the maintenance of the strong shear below the frontal zone for the observed duration.

L.A. Hisscott

Meteorological Department
Ronaldsway Airport, Ballasalla
Isle of Man

551.501.81:551.507.362.2:551.509.56

Meteosat and radar rainfall imagery interpretation on the night of 20/21 November 1986

A.J.Waters

Meteorological Office, Bracknell

Summary

Satellite and radar imagery often reveal striking patterns. Correct interpretation of the imagery can improve weather prediction, especially short-period forecasts. Examples of imagery available in near real time on 20/21 November 1986 are shown, and important signatures highlighted.

1. Introduction

Overnight on the 20/21 November 1986, severe weather, including thunderstorms and heavy rain, occurred in a band some 200 km wide extending from south-west Wales to the eastern English Channel (Fig. 1). A tornado at Swindon around 2330 GMT and a waterspout at Selsey around 0045 GMT caused extensive structural damage. These were examples of some of the mesoscale convective phenomena observed within the circulation of a deepening depression that moved eastwards across England and Wales (Fig. 2). Classically, this could be considered as a 'left exit' development in the diffluent trough ahead of a very strong north-westerly jet (maximum wind around 320° / 160 kn near 280 mb).

There now follows an examination of how the imagery from Meteosat and the UK weather radar network for 2200 GMT on 20 November and 0100 GMT on 21 November (Figs 3 and 4) displayed key signatures that could be interpreted and related to some of the mesoscale phenomena that occurred.

2. Key signatures

The four key signatures considered are line convection and deep convection on the radar imagery, and the dry tongue and comma-shaped cloud area on the Meteosat imagery.

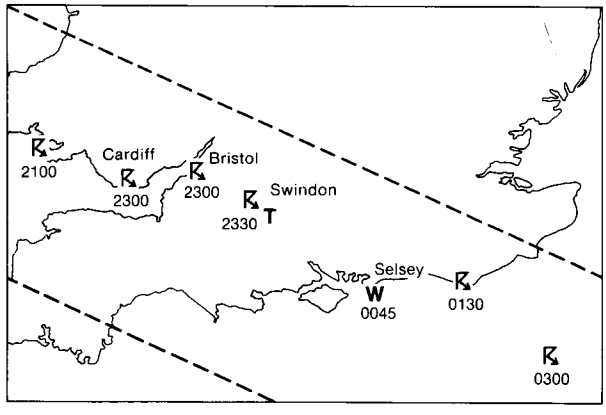

Figure 1. The zone, with approximate boundaries (— — —), in which severe weather was observed overnight on 20/21 November 1986, showing the approximate times of occurrence and positions of thunderstorms (⇘), waterspout (W) and tornado (T).

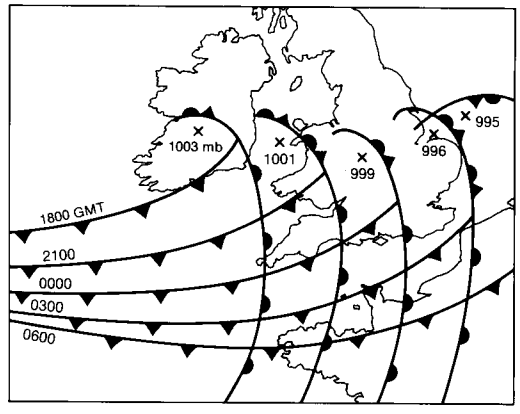

Figure 2. Continuity chart from 1800 GMT on 20 November to 0600 GMT on 21 November 1986, showing the position of the surface fronts and the low pressure centre at 3-hour intervals.

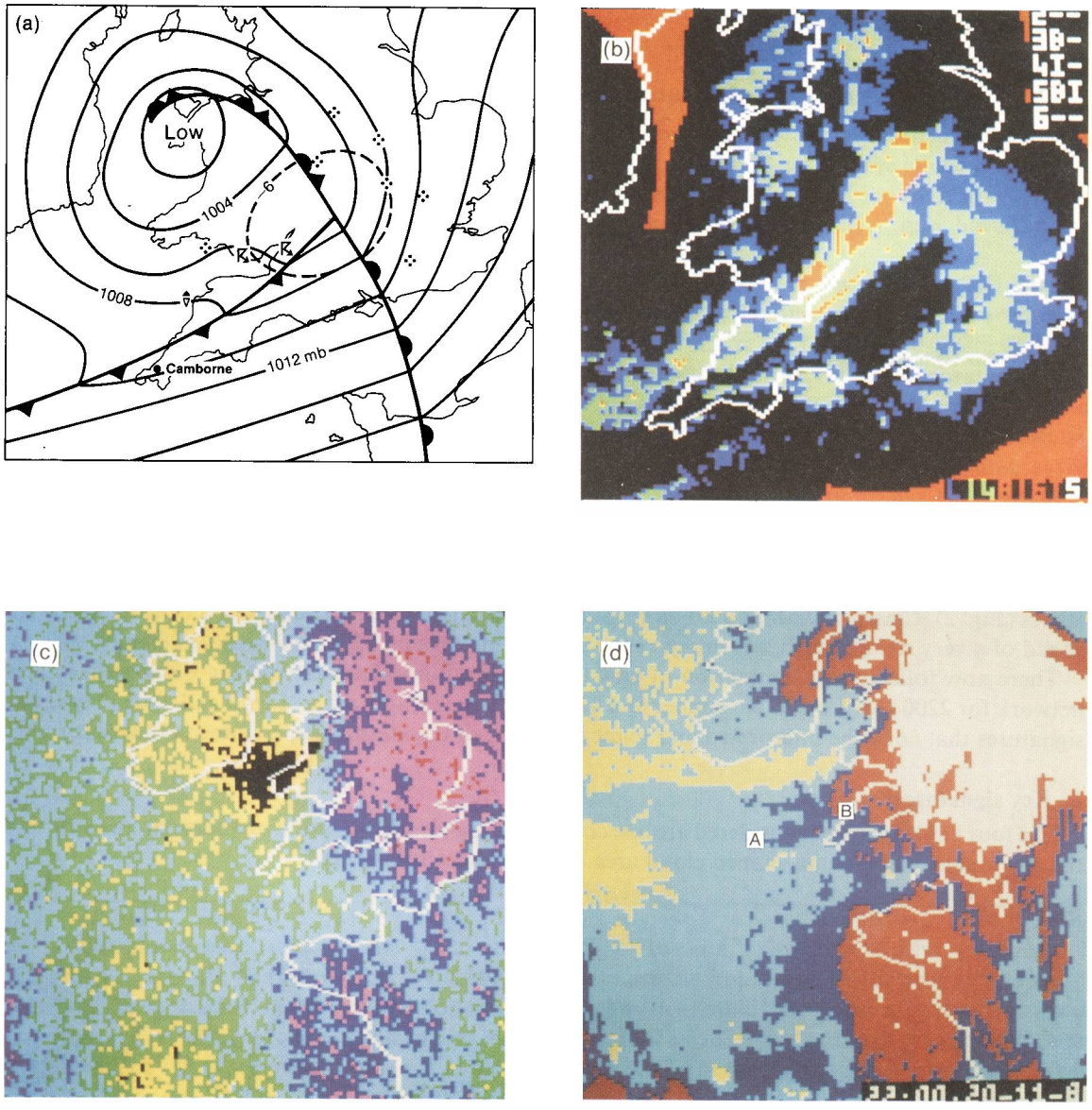

Figure 3. Surface analysis and imagery at 2200 GMT on 20 November 1986. (a) Surface analysis including the −6 mb/3 h isallobar (— — —) and surface observations of heavy precipitation, hail (▲) and thunderstorm (⛈). (b) Rainfall distribution from the UK weather radar network with intensities indicated by colours as follows: blue $\geqslant 0.1$ mm h^{-1}, green $\geqslant 1$ mm h^{-1} and orange $\geqslant 8$ mm h^{-1}. The outer orange areas are spurious and the marks and letters in the top right hand corner refer to the radar sites, calibration adjustment type and bright-band height. For detail on these, and radar display systems in general, see Blackall (1983). (c) Meteosat false-colour water vapour image, black represents the driest and red the moistest air. (d) Meteosat false-colour infra-red image, approximate temperatures indicated by colours as follows: white $\leqslant -40$ °C, red $\leqslant -20$ °C, dark blue $\leqslant -10$ °C, light blue $\leqslant 0$ °C and green > 0 °C.

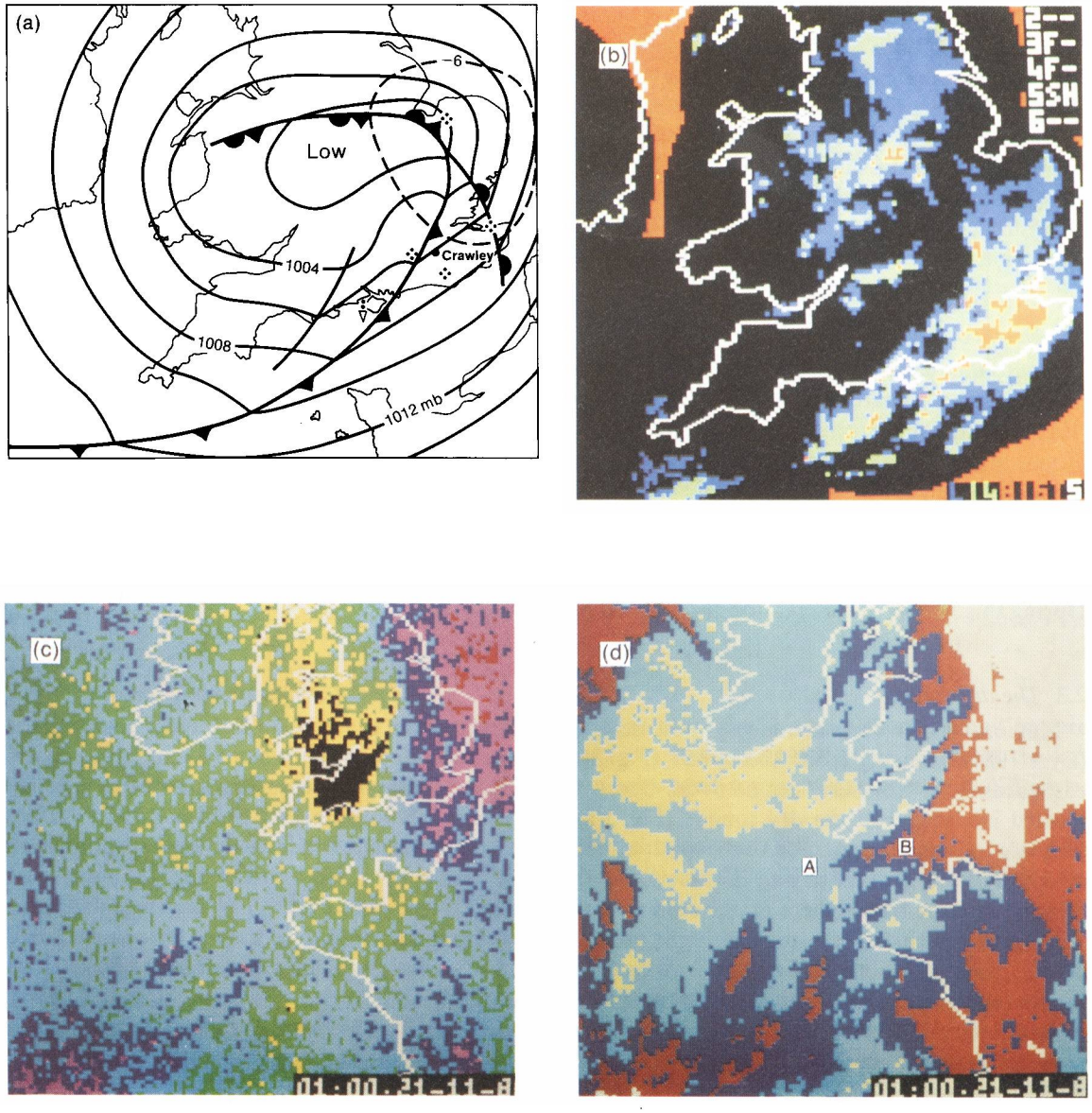

Figure 4. As Fig. 3 but for 0100 GMT on 21 November 1986.

2.1 *Line convection*

Line convection is a relatively shallow phenomenon caused by forced ascent of stable air at an active rearward-sloping cold front (Browning 1985). It can be identified on the 2200 GMT radar rainfall imagery by narrow elements of heavy rainfall ($\geqslant 8$ mm h^{-1}) in a line extending from south-west to north-east just to the east of Bristol (Fig. 3(b)). By recognizing line convection the forecaster can accurately locate the surface cold front. However, because of the shallow nature of the convection, it can only be detected by network radars when within approximately 120 km of individual radar sites. This means that on current network displays line convection may not be continuously observed. However, expansion of the network, with suitably sited radars, should help to reduce this problem.

2.2 *Deep convection*

Just to the rear of the line convection, more extensive areas of heavy rainfall ($\geqslant 8$ mm h^{-1}) present a more striking signature (Fig. 3(b)); note the associated thunderstorm at Cardiff in South Wales (Fig. 3(a)). The movement of these heavy rainfall areas and their decay, and the subsequent development of new areas of heavy rain could be followed on successive pictures. At 0100 GMT most of the heavy rainfall is located over south-east England and the English Channel (Fig. 4(b)).

The Selsey waterspout was probably associated with a small cell (approximately 25 km^2) which was first identified at 2300 GMT about 200 km to the west of Selsey (just east of Torquay). This cell was observable as a discrete entity until around 0100 GMT when it merged with a larger area of heavy rain. During this period of observation the cell had a mean velocity of 250°/65 kn.

2.3 *The dry tongue*

Meteosat water vapour imagery indicates moisture content in the middle and upper troposphere (Eyre 1981). Imagery from 2200 GMT (Fig. 3(c)) reveals a tongue of very dry air extending south-eastwards from Northern Ireland to St. George's Channel. Maximum pressure falls at the surface are located just ahead of the dry tongue (Fig. 3(a)). A similar relationship between the largest surface pressure falls and the position of the dry tongue has been established in other cases such as Young *et al.* (1987). The origin of the dry air in these cases could be traced back to the stratosphere — this air being injected into the troposphere on the cold side of the upper tropospheric jet.

Most of the thunderstorms overnight on 20/21 November occurred over the sea or near exposed coasts. The upper-air sounding for Crawley (Fig. 5(a)) shows that deep convection could be generated by the relatively high prevailing sea surface temperatures (10–13 °C), even within the so-called 'warm sector'. Inland, however, different generating mechanisms would have been required. Triggers could have been supplied by:

(a) orographic lifting,
(b) the surface cold front (SCF) or
(c) the overrunning of low-level air with a relatively high wet-bulb potential temperature (θ_w) near the SCF by drier, lower θ_w air aloft and the subsequent release of potential instability.

The Camborne upper-air sounding (Fig. 5(b)), representative of air just to the rear of the SCF, does show dry air above 650 mb and potential instability between 750 and 600 mb. Note also the very strong winds above 600 mb.

The water vapour imagery for 2200 GMT (Fig. 3(c)) shows the leading edge of the dry air aloft to be just west of the Swindon area. Thunderstorms and the reported tornado occurred in the Swindon area during the following few hours. So, if overrunning is anticipated, the imagery can help identify areas most likely to be affected by deep convection.

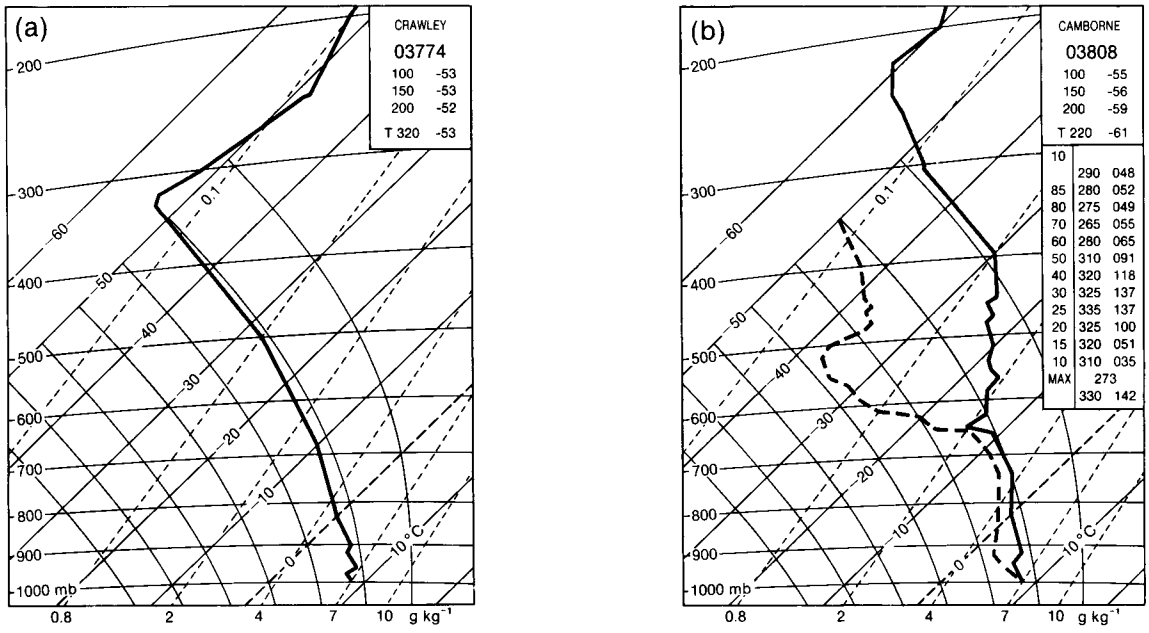

Figure 5. Radiosonde ascents at 0000 GMT on 21 November 1986 for (a) Crawley (humidity data were not available) and (b) Camborne.

2.4 *Comma-shaped cloud area*

A frontal wave that undergoes rapid cyclogenesis has an associated comma-shaped cloud pattern which can be easily identified on infra-red satellite imagery (Carlson 1980). This is one of the key signatures in this case since a large comma-shaped area of cold cloud-top temperature ($\leqslant -20$ °C) can be clearly identified (Fig. 3(d)).

Rapid lowering of cloud-top temperature along a frontal band is indicative of general ascent. This behaviour is apparent in the imagery for 2200 GMT (Fig. 3(d)) and 0100 GMT (Fig. 4(d)) following the path AB as indicated.

3. Conclusions

The forecaster not only has conventional ground-based observations and model products for guidance, but also increasingly has imagery from remote sounding techniques. Good interpretation of signatures revealed by the imagery, examples of which have been highlighted here, allied with some simple airflow models to help in interpretation, should put the forecaster in a better position to produce more accurate forecasts, especially in the short term.

References

Blackall, R.M. 1983 Weather radar systems displays (Jasmin users guide).(Unpublished, copy available in the National Meteorological Library, Bracknell.)

Browning, K.A. 1985 Conceptual models of precipitation systems. *Meteorol Mag*, **114**, 293–319.

Carlson, T.N. 1980 Airflow through mid latitude cyclones and the comma cloud pattern. *Mon Weather Rev*, **108**, 1498–1509.

Eyre, J.R. 1981 Meteosat water vapour imagery. *Meteorol Mag*, **110**, 345–351.

Young, M.V., Monk, G.A. and Browning, K.A. (1987) Interpretation of satellite imagery of a rapidly deepening cyclone. (Submitted to *Q J R Meteorol Soc.*)

Reviews

Chemistry of atmospheres: an introduction to the chemistry of the atmospheres of earth, the planets and their satellites, by Richard P. Wayne. 160 mm × 240 mm, pp. xii + 361, *illus.* Oxford, Clarendon Press, 1985. Price £30.00 (hardback), £14.50 (paperback).

In recent years there have been many textbooks addressing a wide variety of aspects in atmospheric science. This particular book concerns itself specifically with the chemistry of atmospheres — mainly the terrestrial atmosphere but not exclusively so. The author is a physical chemist and while the approach of the book reflects this, it seems designed not to be restricted to those with chemistry backgrounds. The chapters each give overviews of particular aspects of atmospheric chemistry and related areas, and each ends with a fairly extensive bibliography which provides a very useful introduction to those wishing to follow up particular topics. The contents of the chapters reflect the rapidly advancing state of atmospheric chemistry and generally appear up to date. One point of possible concern is that in order to encompass the admittedly wide scope of this book, some of the discussions have been abbreviated or simplified to the point where prior knowledge of the issue in question is desirable or necessary. One pleasing aspect, however, is that the author does (for example in Chapter 9 on the evolution of atmospheres) discuss wider issues than pure chemistry and readers are, for example, encouraged to consider the implications of books such as *Gaia. A new look at life on earth* (Lovelock 1979)*.

Chapter 1 introduces the terrestrial atmosphere to the reader, highlighting specific processes which play or have played significant roles in creating and maintaining the present atmosphere — even heterogeneous chemistry, a subject of some topical interest, is mentioned in passing.

Chapter 2 describes, using basic physical laws, how the temperature and pressure structure of the terrestrial atmosphere arises, with a quite lengthy discussion of the role of radiation in the earth's atmosphere. A minor blemish is that $\sec^2\theta$ on page 49 should in fact be $\sec\theta$. There then follow sections on transport and winds. In the former the rather superficial discussion ranges from vertical eddy diffusion coefficients to tropopause folding in less than a page — certainly an example of excessive compression! The chapter ends with sections on particle nucleation and scattering.

Chapter 3 outlines from first principles the basic photochemical processes using, usefully, examples from the terrestrial atmosphere. The discussions of chemical kinetics are extensive but the weakness of this chapter is the section (about 3 pages) on numerical modelling which is unhelpfully brief.

Chapters 4 and 5 deal with the chemistry of the lower and middle terrestrial atmosphere. Chapter 4 addresses the important subject of ozone in the earth's stratosphere; again a wide ranging but brief résumé. One concern is that between pages 116 and 120 'odd oxygen' becomes 'ozone' and perhaps in consequence the height dependence of the odd oxygen destruction reaction (page 118) is ignored. This is followed by an extensive discussion of catalytic ozone destruction, and the likelihood of man perturbing the ozone balance in the stratosphere is clearly presented. In keeping with the general tone of the book, it might have been pointed out in the section 'Comparison of experiment with theory' that even though 'the general pattern of stratospheric chemistry' is 'well understood' (page 139) there is a 30% discrepancy between modelled and observed ozone in the upper stratosphere — a region where the chemical time constants are much shorter than those for transport, and where the models might be expected to perform in some sense 'best'. Chapter 5 deals with chemistry in the troposphere. The format is much the same as Chapter 4. There are sections describing sulphur chemistry (important in so-called 'acid rain') and photochemical smog. In the latter it would have been worth emphasizing that much of the apparent

* Lovelock, J.E.; *Gaia. A new look at life on earth.* Oxford University Press, Oxford, 1979.

diurnal variations of ground-level ozone can be attributed to meteorological rather than chemical causes.

The upper atmosphere is considered in Chapters 6 and 7. Chapter 6 discusses the role of ions and ion chemistry in various atmospheric regions. It is interesting in the light of recent depletions in Antarctic ozone that the possible importance of ion catalysed reactions in the low stratosphere and troposphere is mentioned briefly. Chapter 7 is concerned with the airglow. There is a useful discussion of various excitation mechanisms, although it does not seem necessary to introduce the complications of Einstein 'A' coefficients (page 263).

Chapter 8 discusses extra-terrestrial atmospheres — in particular their chemical composition on Venus, Mars, the giant planets and the one satellite possessing a significant atmosphere, Titan. This chapter is interesting because it not only describes the composition of each in turn, but also attempts to assess, in the light of the photochemistry described earlier, what chemical reactions might be important in the different regimes.

Chapter 9 considers the evolution and possible future trends of planetary atmospheres, mainly the earth's. The complexity of the role that man can play in altering atmospheric composition and ultimately climate is well illustrated and, as far as is possible in five pages, the climatic consequences are assessed.

Overall, the book provides a useful introduction to atmospheric chemistry. The author has attempted to put atmospheric chemistry into a wider context and in this he has been largely successful. It is perhaps inevitable in a book of this scope that some topics, for example meteorology and dynamics, are treated rather sketchily. However, the fairly extensive bibliographies should enable this problem to be, to some extent, overcome. Overall the book is to be recommended.

R.L. Jones

Notes on numerical fluid mechanics, Volume 13: Proceedings of the sixth GAMM-Conference on numerical methods in fluid mechanics, edited by D. Rues and W. Kordulla. 155 mm × 230 mm, pp. x + 408, *illus.* Braunschweig/ Wiesbaden, Friedr. Vieweg and Sohn, 1986. Price £31.00.

This volume contains the 51 papers which were presented at the sixth GAMM (Gesellschaft für Angewandte Mathematik und Mechanik) Conference on numerical methods in fluid mechanics held in Göttingen, Federal Republic of Germany, in September 1985. This conference is organized every two years at different places in Western Europe. The papers cover a broad range of topics, from the mathematical development and investigation of algorithms to their application to fluid mechanical problems in acoustics, aerodynamics, car aerodynamics, gas dynamics, hydrodynamics, meteorology, oceanography,turbo-machinery, etc. This volume also includes a brief report on the GAMM workshop 'The efficient use of vector computers with emphasis on computational fluid dynamics' which followed the conference.

There are only two papers specifically on meteorological problems, by Th.L. van Stijn and F.T.M. Nieuwstadt of the Royal Netherlands Meteorological Institute on 'Large eddy simulation of atmospheric turbulence' and by H. Volkert and U. Schumann of Deutsche Forschungs — und Versuchsanstalt für Luft — und Raumfahrt, Oberpfaffenhofen, on 'Development of an atmospheric mesoscale model'. The first of these papers presents a number of interesting computations as well as a brief description of the model used. The second paper is part of a series of contributions to these conferences and it is very uninformative read on its own.

The remainder of the volume can be roughly divided into papers on algorithms in general and papers on applications, mostly in aerodynamics. The same bias is clear in the papers on algorithms. Nearly all discuss finite difference or finite volume methods. The latter are finite difference schemes formulated to ensure satisfaction of integrated conservation requirements. A recurrent theme is the need to compute sharp discontinuities without generating spurious overshoots. Quite successful methods are now available for doing this in two dimensions in the presence of strong but steady shock waves. Interest in this area of atmospheric modelling is growing with the increasing attention given to very-high-resolution modelling. Many of the applications are to steady flows and there is a great deal of work on design of grids that most accurately represent the flow features. This approach is not common in atmospheric modelling since the use of an irregular grid to represent an unsteady flow often causes large errors.

Even though the papers in the volume are restricted to a maximum of approximately eight pages, a high proportion of them are understandable by anyone with a reasonable knowledge of numerical methods. There has always been a gap between numerical modelling in meteorology and the mainstream of computational fluid dynamics. Though this probably reflects genuinely large differences in the problems to be solved, there is much that meteorologists can learn from experiences in other fields. There is a considerable interchange of techniques used in modelling turbulent flows but the similarity between methods of modelling low speed flows, e.g. past motor cars, with those for modelling certain atmospheric structures has not been fully exploited.

M.J.P. Cullen

Prediction of solar radiation on inclined surfaces, edited by J.K. Page. 165 mm × 238 mm, pp. xii + 459, *illus.* Dordrecht, D. Reidel Publishing Company, 1986. Price £59.50, US $85.00, Dfl 180.00.

This book describes the results of several years of collaborative research, involving a number of groups within the European Community, aimed at providing a comprehensive set of techniques for calculating solar radiation on inclined surfaces. The declared objective is to help solar energy practitioners in all fields, with methods presented in a practical form that can be used by designers. These have been tested for many locations and are intended to be widely applicable.

Modellers of solar radiation fall mainly into two camps. Those concerned with radiation schemes within numerical climatological or synoptic models tend to subdivide the solar spectrum into narrower bandwidths which can be dealt with by approximations based on the full radiative transfer equations; those concerned with solar radiation as a source of energy, mainly for buildings and agriculture with both passive solar heating and active energy generation, usually require site-specific and climatological data. The latter group tend to deal with broad-band radiation components with complex pragmatic relations depending upon sunshine amount and other readily available observations. This book lies entirely within the second category and describes in detail both these pragmatic relations and the ideas behind them.

A brief theoretical background is provided in the text, with a major proportion of the volume being given up to tables and diagrams describing the comparison of observed data with various models' results. The early chapters describe the development of a technique for predicting solar radiation on a horizontal surface under cloudless skies. Here the major uncertainty lies in specifying the turbidity, i.e. the attenuation due to aerosol, which varies considerably both with location and from day to day. The next section displays recent observations of the angular distribution of the radiance of cloudless skies and indicates how these data may be applied to estimating clear sky radiation on inclined surfaces. A method of prediction for overcast days is then described, demonstrating the considerable statistical fluctuations due to the presence of clouds. The final chapters catalogue the synthesis of these results into techniques for predicting mean solar radiation on inclined surfaces.

This volume provides a wealth of information for the solar energy user interested in the detailed availability of solar radiation, using the most recent techniques tried and tested with modern data, for many European locations. In particular a useful guide is given to estimating the turbidity for areas where conventional data are absent. A series of look-up tables can be consulted which simplify the process of determining radiation values for arbitrary orientations of the surface. A number of appendices include useful supplementary data concerning the sun–earth geometry, day length and other radiation related factors.

The main drawback with this book lies in the sheer amount of information presented and in its organization, perhaps unavoidable in a subject which relies heavily on establishing numerous empirical dependences, with several authors contributing to the final product. It would have been useful to separate more clearly the verification of methods from their application in calculating solar radiation in practice. The casual user of solar radiation data should be directed towards the maps of radiation on horizontal and inclined surfaces already prepared by the methods described (*CEC European Solar Radiation Atlas, Vols I and II*). It is difficult to decide whether the complexity of the presented techniques is justified by the accuracy required by most users, particularly with the uncertainties in sunshine amount and turbidity. This is compounded by the complication that different criteria are needed for different averaging periods, as is common in climatological problems. It seems unlikely that the bulk of the detailed developmental results would be of interest to any but the most specialized worker. Summarizing, this book will serve as a useful reference work for those in the solar energy community who are interested in the details of simulating solar radiation climatology, but not as an easily accessible source for the uncommitted reader.

F. Rawlins

Books received

The listing of books under this heading does not preclude a review in the Meteorological Magazine at a later date.

Basic meteorology, a physical outline, by J.F.R. McIlveen (Wokingham, Van Nostrand Reinhold (UK) Co. Ltd, 1986. £15.95 (paperback only)) attempts to merge the two usual approaches to meteorology: describing the facts of atmospheric behaviour and explaining the physical mechanism involved. It is intended for students during the first two years of relevant degree courses, and the author is an experienced lecturer on the subject.

The uncertainty business, by W.J. Maunder (London, Methuen and Co. Ltd, 1986. £45.00) argues that weather information is a valuable commodity for decision-making in many key areas of human activity. A manifesto is issued for the development of new areas of research, requiring the skills from several disciplines.

Climate, weather and Irish agriculture, edited by T. Keane (Dublin, Mount Salus Press Ltd, 1986. Ir. £9.95 (paperback), Ir. £14.95 (hardback)) details the relationship between Irish weather and agriculture. There are four main strands: climate and weather, soil management, crop production and animal production. In each area the most recent research is included and many subjects which were only in scattered sources are drawn together.

Satellite photograph — 15 December 1986 at 0548 GMT

The NOAA-9 infra-red image received and displayed via the Meteorological Office HERMES system, shows a distinctive cloud whirl associated with an intense Atlantic depression of unusual depth. The Central Forecasting Office (CFO) surface analysis for 0600 GMT suggested the depth to be 920 mb with an observed pressure of 926.6 mb reported near the centre. The minimum central pressure of the low was 916 mb (6 hours earlier) following 36 hours of rapid cyclogenesis as two separate centres combined, accompanied by a pressure fall of 70–80 mb.

The occluded front, marked in the CFO analysis as terminating west of the depression centre, is seen in the image to spiral into the centre. South of the depression centre, the depth and scale of the convection (originating in the Labrador region) increases progressively, such that over the warm waters of the central Atlantic considerable cumulonimbus cloud is present, with anvils shearing off ahead and to the left of the track of the convection cells in the strong upper winds, within a region of cold air advection.

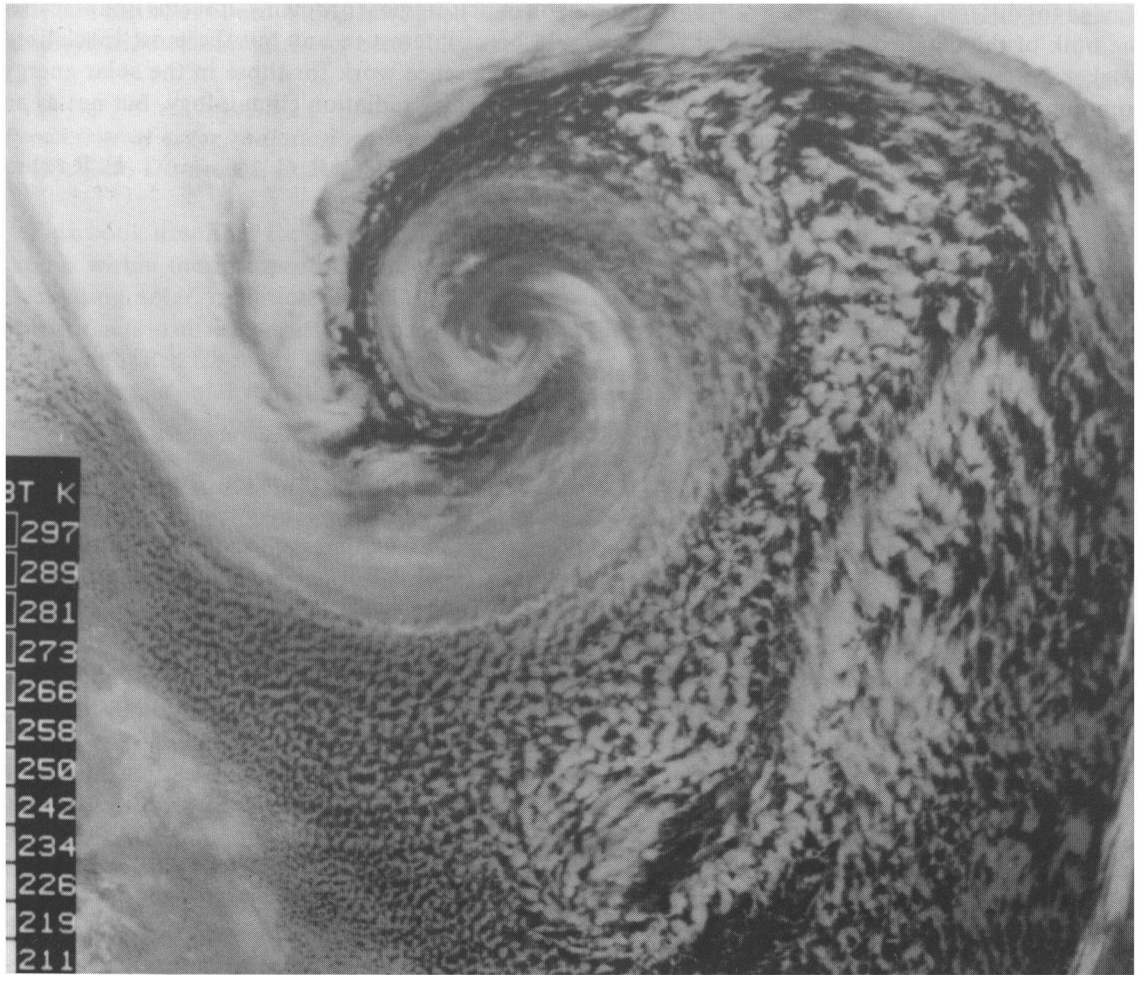

Meteorological Magazine

GUIDE TO AUTHORS

Content

Articles on all aspects of meteorology are welcomed, particularly those which describe the results of research in applied meteorology or the development of practical forecasting techniques.

Preparation and submission of articles

Articles for publication and all other communications for the Editor should be addressed to the Director-General, Meteorological Office, London Road, Bracknell, Berkshire RG12 2SZ and marked 'For *Meteorological Magazine*'.

Articles, which must be in English, should be typed, double-spaced with wide margins, on one side only of A4-size paper. Tables, references and figure captions should be typed separately.

Spelling should conform to the preferred spelling in the *Concise Oxford Dictionary*.

References should be made using the Harvard system (author, date) and full details should be given at the end of the text. If a document referred to is unpublished, details must be given of the library where it may be seen. Documents which are not available to enquirers must not be referred to.

Tables should be numbered using roman numerals and provided with headings. We consider vertical and horizontal rules to be unnecessary in a well-designed table; spaces should be used instead.

Mathematical notation should be written with extreme care. Particular care should be taken to differentiate between Greek letters and Roman letters for which they could be mistaken. Double subscripts and superscripts should be avoided, as they are difficult to typeset and difficult to read. Keep notation as simple as possible; this makes typesetting quicker and therefore cheaper, and reduces the possibility of error. Further guidance is given in BS1991: Part 1: 1976 and *Quantities, Units and Symbols* published by the Royal Society.

Illustrations

Diagrams must be supplied either drawn to professional standards or drawn clearly, preferably in ink. They should be about 1½ to 3 times the final printed size and should not contain any unnecessary or irrelevant details. Any symbols and lettering must be large enough to remain legible after reduction. Explanatory text should not appear on the diagram itself but in the caption. Captions should be typed on a separate sheet of paper and should, as far as possible, explain the meanings of the diagrams without the reader having to refer to the text.

Sharp monochrome photographs on glossy paper are preferred: colour prints are acceptable but the use of colour within the magazine is at the Editor's discretion. In either case contrast should be sufficient to ensure satisfactory reproduction.

Units

SI units, or units approved by WMO, should be used.

Copyright

Authors wishing to retain copyright for themselves or for their sponsors should inform the Editor when they submit contributions which will otherwise become UK Crown copyright by right of first publication.

It is the responsibility of authors to obtain clearance for any copyright material they wish to use before submitting it for publication.

Free copies

Three free copies of the magazine are provided for authors of articles published in it. Separate offprints for each article are not provided.

Meteorological Magazine

March 1987

Vol. 116
No. 1376

CONTENTS

Contributions: it is requested that all communications to the Editor and books for review be addressed to the Director-General, Meteorological Office, London Road, Bracknell, Berkshire RG12 2SZ, and marked 'For *Meteorological Magazine*'. Contributors are asked to comply with the guidelines given in the *Guide to authors* which appears on the inside back cover. The responsibility for facts and opinions expressed in the signed articles and letters published in *Meteorological Magazine* rests with their respective authors. Authors wishing to retain copyright for themselves or for their sponsors should inform the Editor when submitting contributions which will otherwise become UK Crown copyright by right of first publication.

Subscriptions: Annual subscription £27.00 including postage; individual copies £2.30 including postage. Applications for postal subscriptions should be made to HMSO, PO Box 276, London SW8 5DT; subscription enquiries 01–211 8667.

Back numbers: Full-size reprints of Vols 1–75 (1866–1940) are available from Johnson Reprint Co. Ltd, 24–28 Oval Road, London NW1 7DX. Complete volumes of *Meteorological Magazine* commencing with volume 54 are available on microfilm from University Microfilms International, 18 Bedford Row, London WC1R 4EJ. Information on microfiche issues is available from Kraus Microfiche, Rte 100, Milwood, NY 10546, USA.

ISBN 0 11 727967 6

ISSN 0026–1149

Printed for HER MAJESTY'S STATIONERY OFFICE
by Delco Printing Co.Ltd. 3/87 Dd. 739131 C1400